



Elettra
Sincrotrone
Trieste

Optical Component for Synchrotron Light

*School on Synchrotron
and Free-Electron-Laser Methods
for Multidisciplinary Applications*

ICTP, 7th May -18th May 2018



*Edoardo Busetto & Luca Rebuffi - MVO Group
Elettra - Sincrotrone Trieste S.C.p.A.*

ICTP, Grignano (TS), 07/05/2018



Optical components for SL: mirrors and monochromators

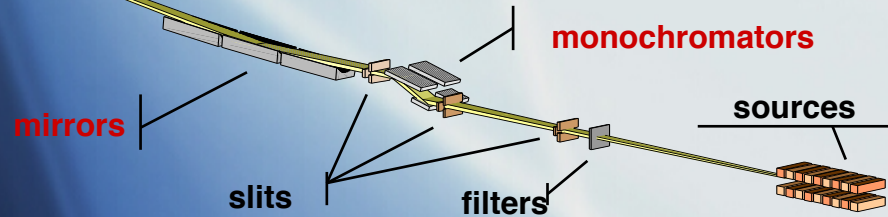
low emittance electrons beam produces a high brilliance x-ray photons beam.

“ ...The finite quality and the fundamental limits of the optical components increase the emittance of the beam.....

The main aim of the optical design consists on minimizing the inevitable beam degradation...”

Jean Susini “Design parameters for hard x-ray mirrors: the ESRF case”
OPTICAL ENGINEERING/February 1995/Vol. 34 2/361

detectors

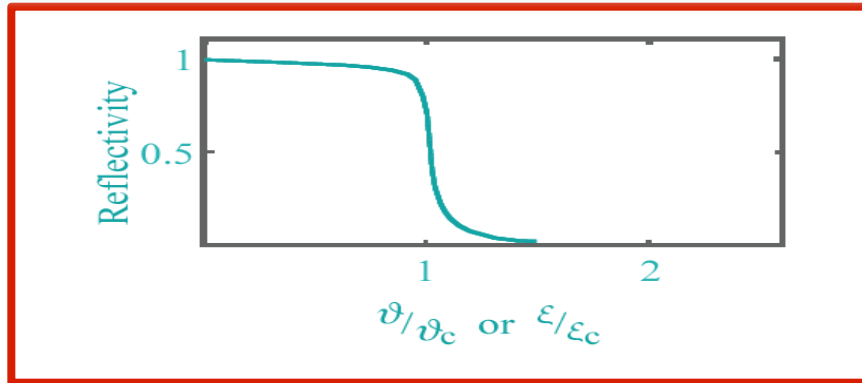


The most important optical elements for a beamline:

- mirrors
- monochromators

Optical components for SL Mirrors: total reflection

If we consider θ as the angle between the incoming radiation and the mirror surface (grazing angle), the x-ray beam will be totally reflected when $\theta < \theta_c$

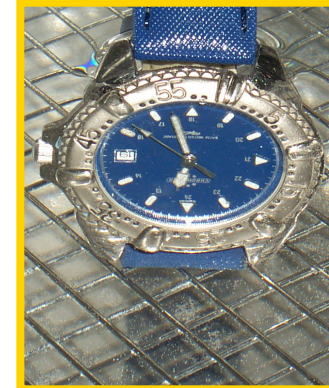


For x – rays the refraction index is $n = 1 - \delta$
where $0 < \delta < 1$, and therefore $0 < n < 1$

$$\theta < \theta_c$$

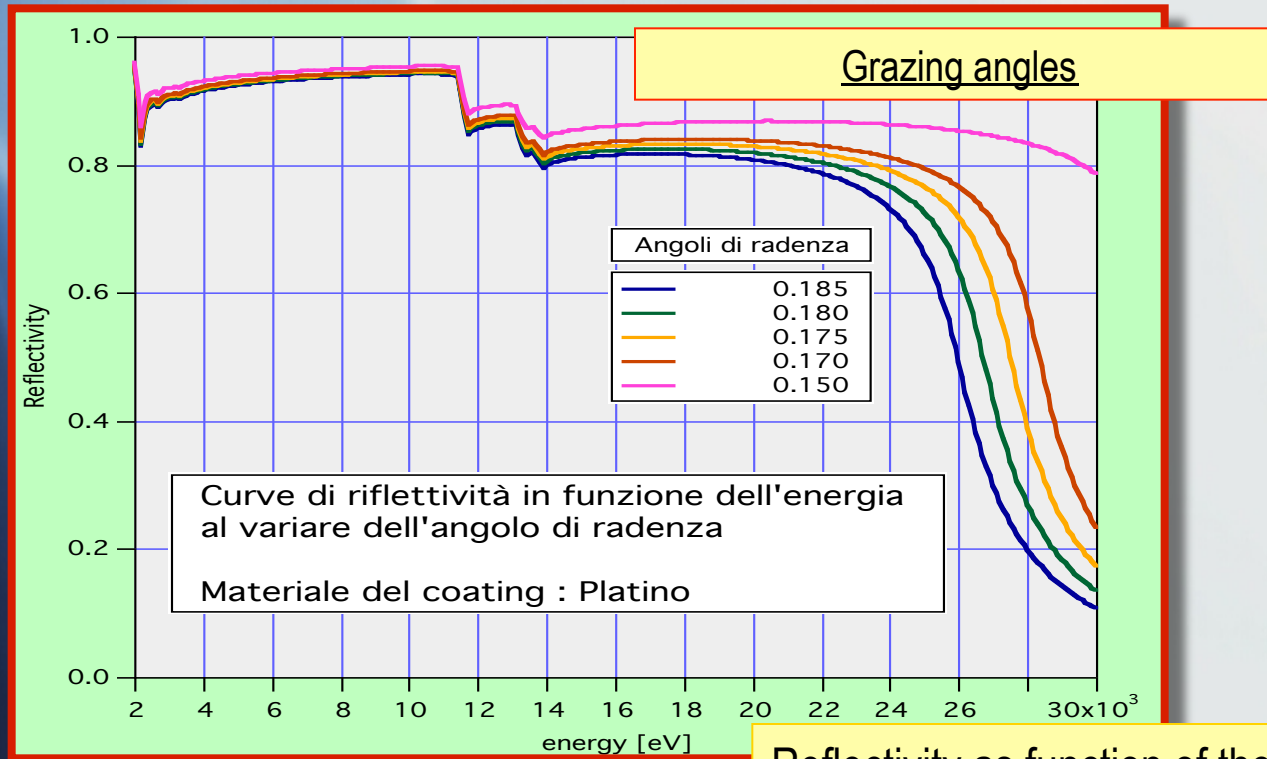
$$\theta = \theta_c$$

$$\theta > \theta_c$$



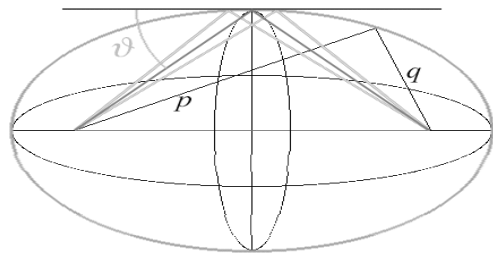
Optical components for SL Mirrors: total reflection

$$\theta_c = 1.66 \lambda [\text{\AA}] (\rho)^{1/2} [\text{g/cm}^3]$$

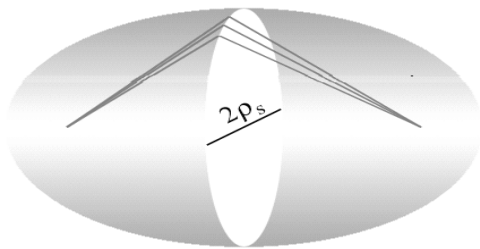


Optical components for SL Mirrors: focusing

Ellipsoidal surface



Tangential focusing



Sagittal focusing

Best approximation circle

$$\rho_{tangential} = 2f / \sin \vartheta$$

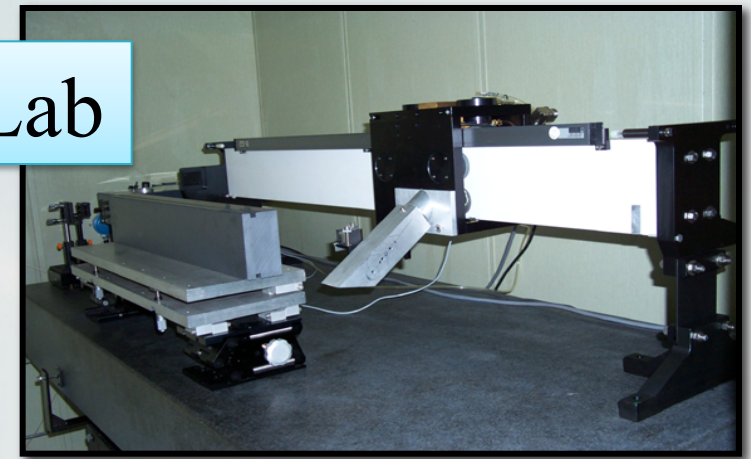
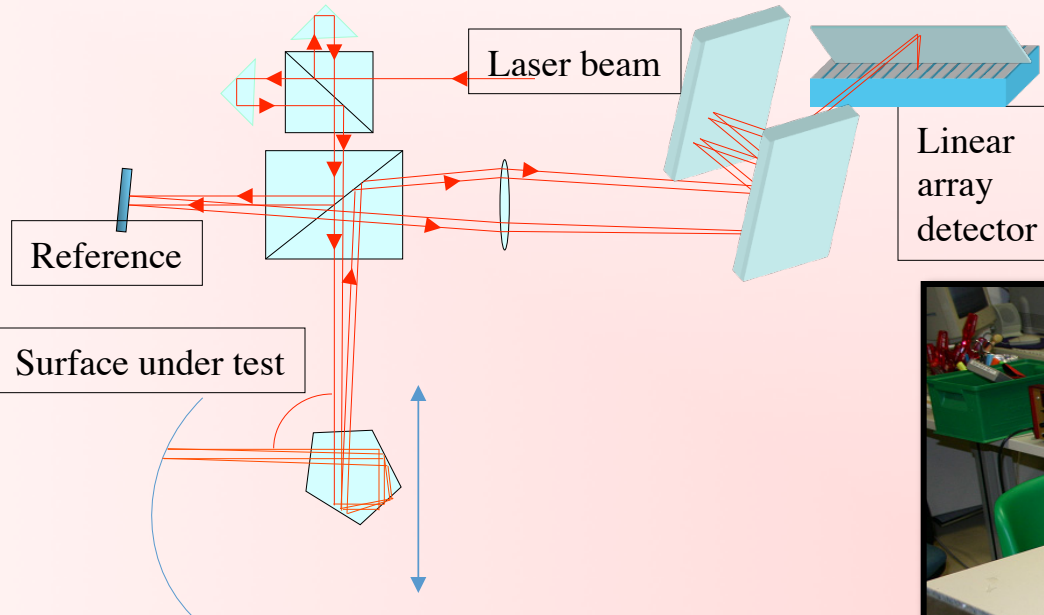
an ideal focusing mirror will focus a point source into another point according to the formula
 $1/q + 1/p = 1/f$

$$\rho_{sagittal} = 2f \sin \vartheta$$

- Bendin magnet
- Extended source (wiggler and undulators)

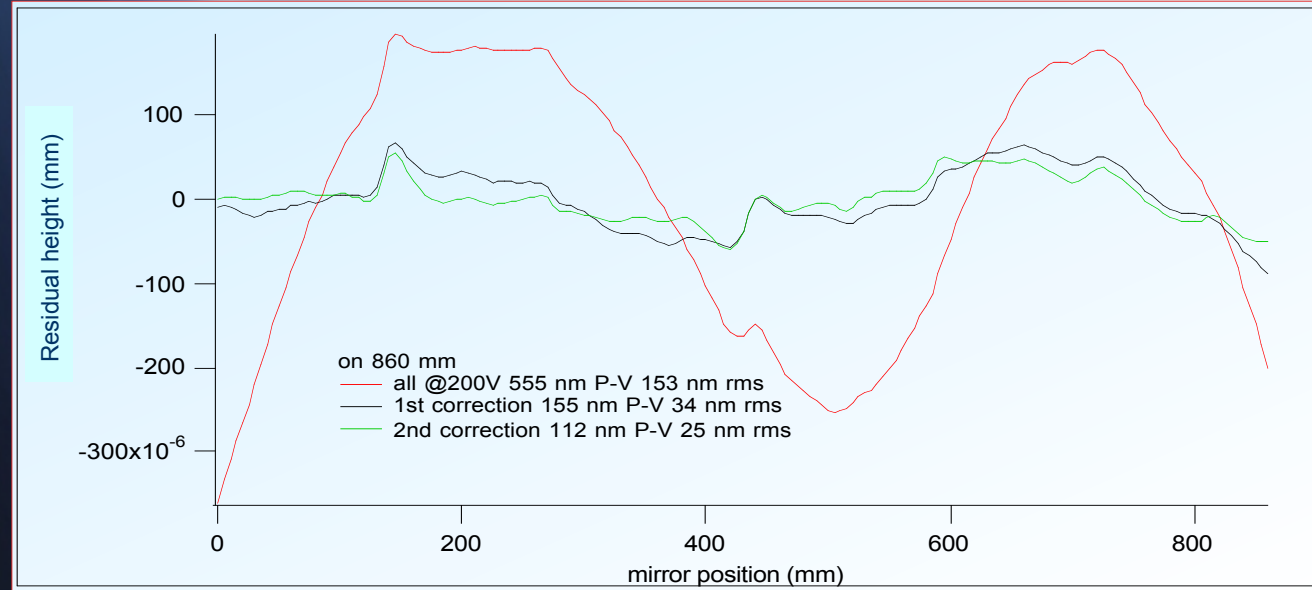
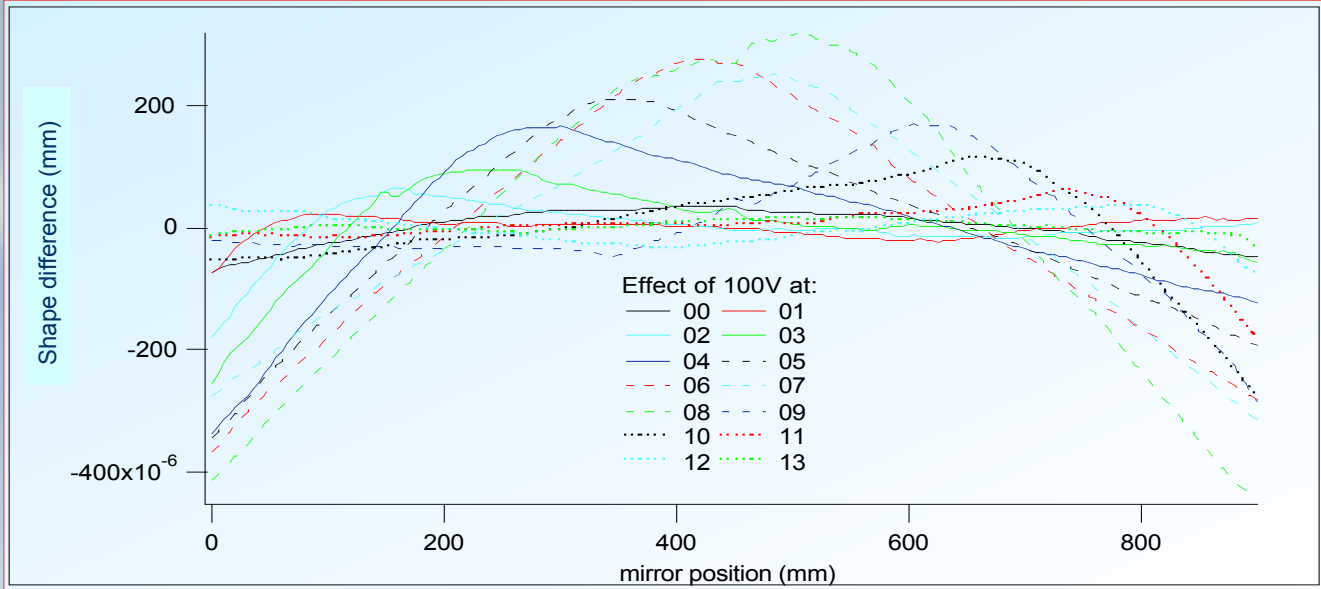


Optical Metrology Lab





Elettra
Sincrotrone
Trieste



13 active mirror sections
10 minutes / measurement
Total time > 130 minutes



voltage stability



Edoardo Busetto & Luca Rebuffi - MVO Group
Elettra - Sincrotrone Trieste S.C.p.A.

Optical Metrology Lab

ICTP, Grignano (TS), 07/05/2018





In last 10 years

- 200 - 400 mm long flat mirrors:
from $\sim 1 \mu\text{rad}$ to $\sim 0.2 \mu\text{rad}$ rms
Ion beam figuring (IBF) now almost normally applied
- curved mirrors
 $R=100 \text{ m}$, 100 mm long : **0.45 μrad** rms
Toroid $R=300 \text{ m}$, $r = 100 \text{ mm}$, 200mm long : **0.5 μrad** rms
- High quality ellipses
IBF finished, 200mm long: **0.8/1 μrad** rms from best ellipse
 $F=900\text{mm} / 500\text{mm} @ 2.5 / 2 \text{ deg}$
Fluid jet polishing ,100 mm long: **0.07 μrad** rms from best ellipse
 $F=180 \text{ mm} / 280\text{mm} @ 2.5/ 3 \text{ mrad}$





Goals for the next 10 years

Mirror shape errors

Slope errors < 50 nrad rms from best shape : flat and moderate curvature
height errors < 0.1 nm rms

Improvement of figuring technology

Convergence of iterative figuring process

Development of fast accurate metrology procedures

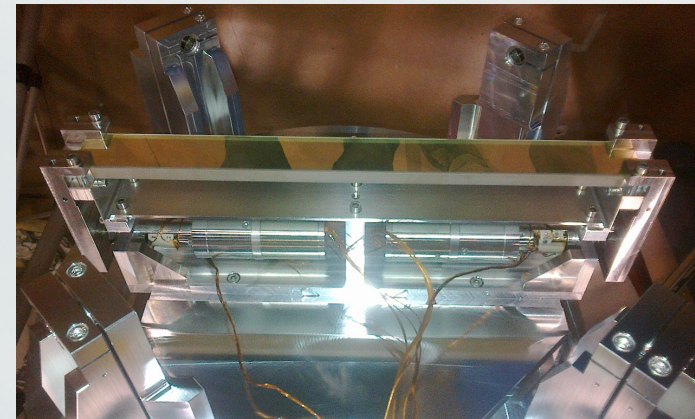
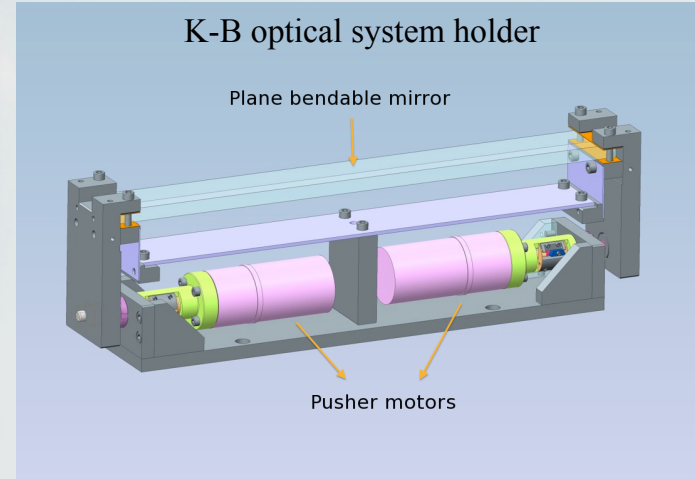
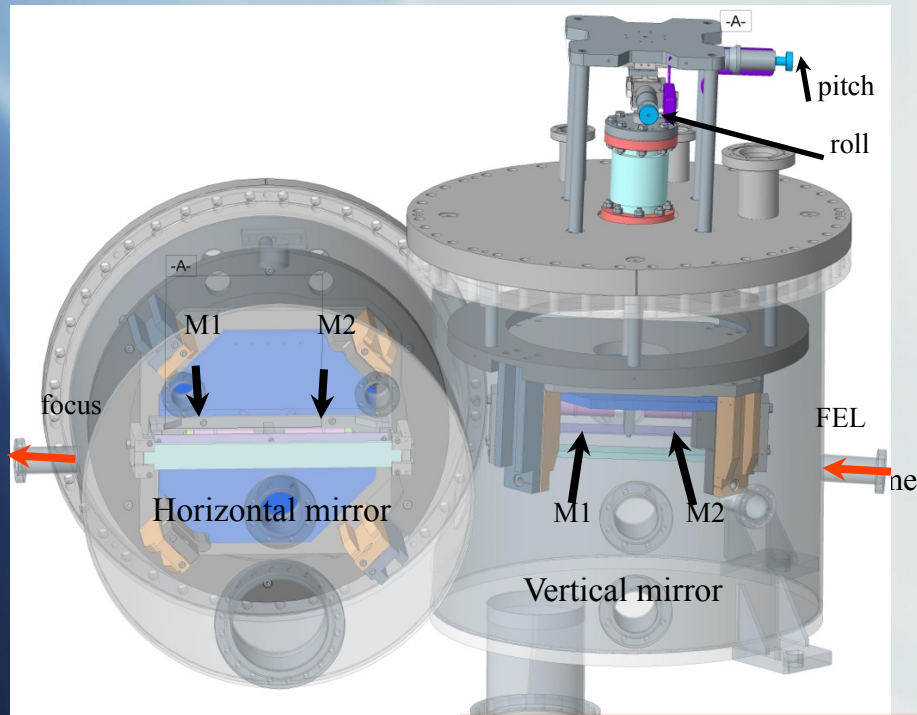
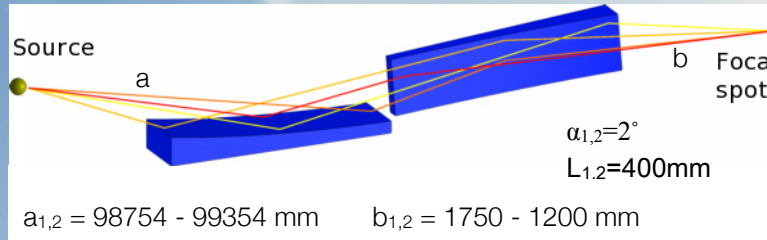
At synchrotrons

At manufacturers





Optical components for SL Mirrors: figure errors modification



K-B active optical system – DiProI

*L. Raimondi et al. Status of the K-B bendable optics at FERMI@Elettra FEL
Proc. Of SPIE Vol.9208 920804-1*



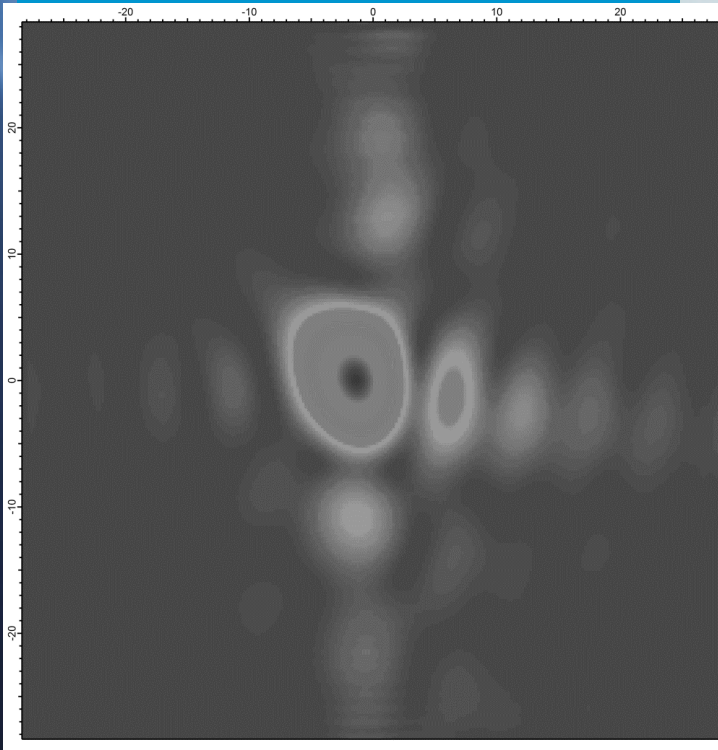


Elettra
Sincrotrone
Trieste

Focal spot simulations from metrology

Reconstruction from Hartmann WFS data

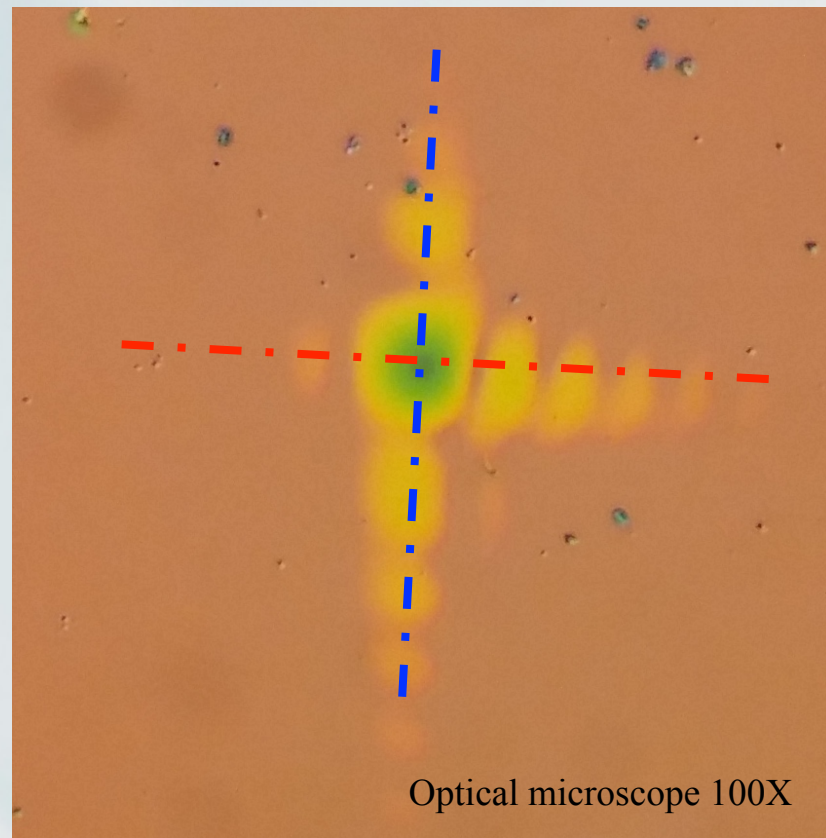
https://en.wikipedia.org/wiki/Shack-Hartmann_wavefront_sensor



x6.5 μm^2

■KAOS PMMA indentation / WFS measurement

PMMA ablation imprint



Good agreement between in-house reconstruction, PMMA, simulations (WISE, SRW)

ICTP, Grignano (TS), 07/05/2018



Edoardo Busetto & Luca Rebuffi - MVO Group
Elettra - Sincrotrone Trieste S.C.p.A.





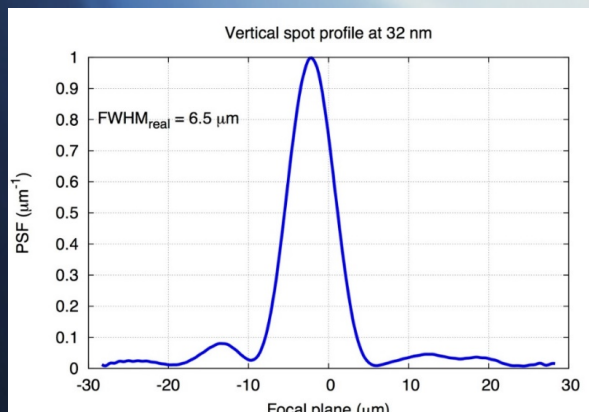
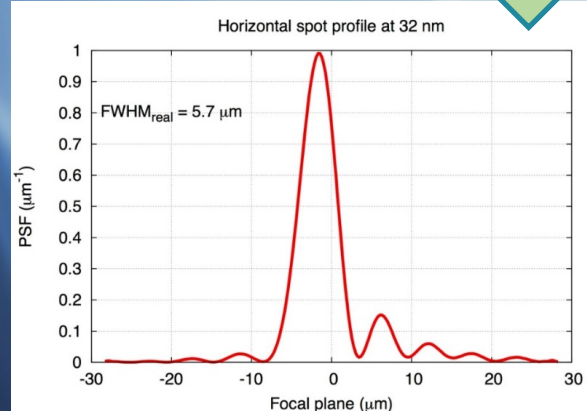
Elettra
Sincrotrone
Trieste

Focal spot simulations from metrology

Profilometry at best curvature (LTP)



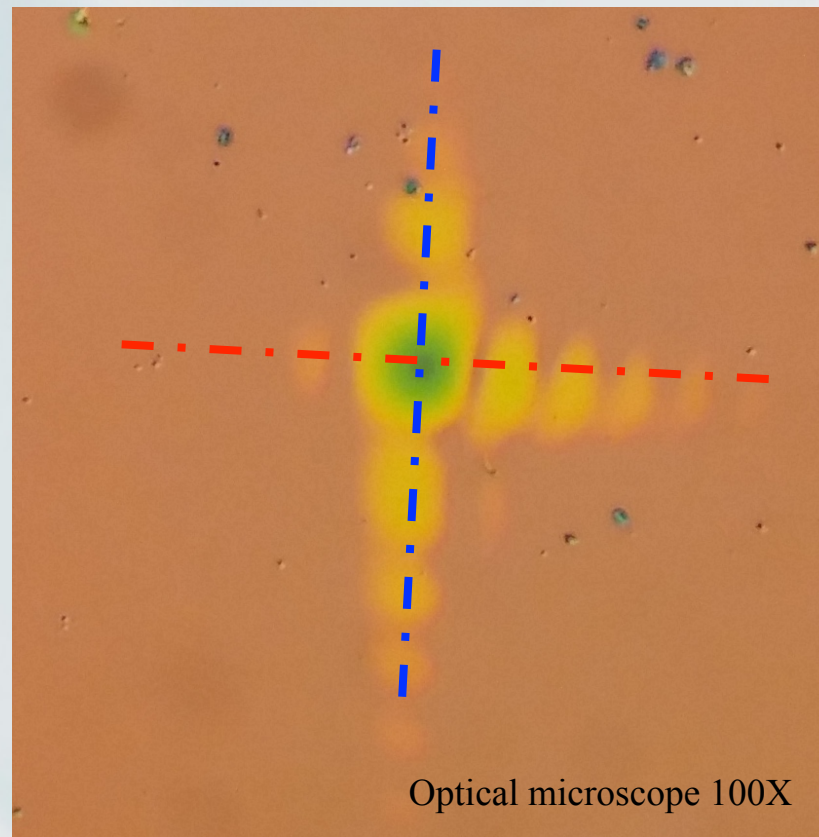
Simulations (WISE, SRW)



■KAOS

PMMA indentation / WFS measurement

PMMA ablation imprint



Optical microscope 100X

Good agreement between in-house reconstruction, PMMA, simulations (WISE, SRW)

ICTP, Grignano (TS), 07/05/2018



Edoardo Busetto & Luca Rebuffi - MVO Group
Elettra - Sincrotrone Trieste S.C.p.A.

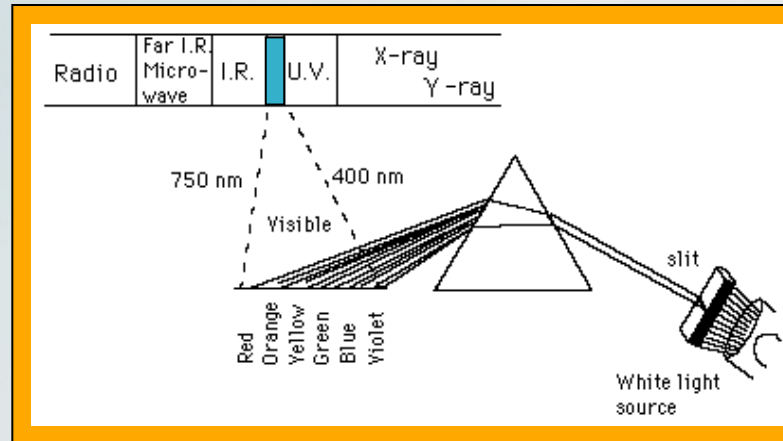


Optical component for SL: Visible light monochromators

Dispersion of radiation through the matter: the RIFRACTION

Visible radiation optical PRISM

The glass refraction index depends on the radiation wavelength, the optical prism splits the visible radiation as function of the energy



We can sample the dispersed beam with a slit selecting part of it. The spectral resolution will depend on the glass refraction index n , on the slit aperture and on the distance between slits and the optical prism.



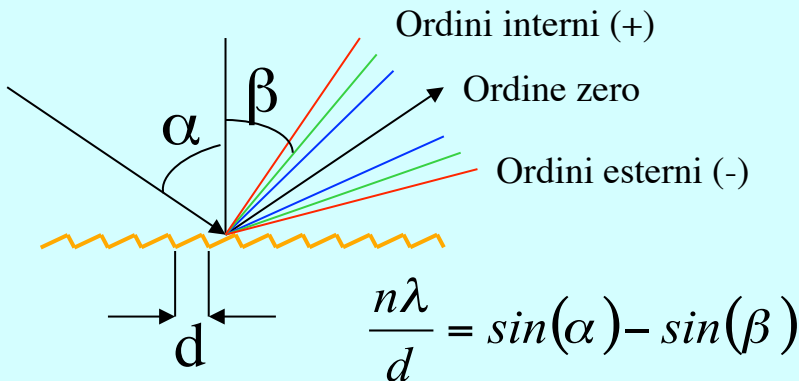
Optical component for SL: Soft x-rays monochromators

Dispersion of radiation from a periodic structured surface:
the surface DIFFRACTION



GRATINGS

Microwave	I.R.	Visible	U.V.	Soft X-ray	Hard X-ray
-----------	------	---------	------	------------	------------



The optical surface is machined with particular periodic structures that are origin of interference phenomena with the incoming radiation

Optical component for SL: Hard x-rays monochromators

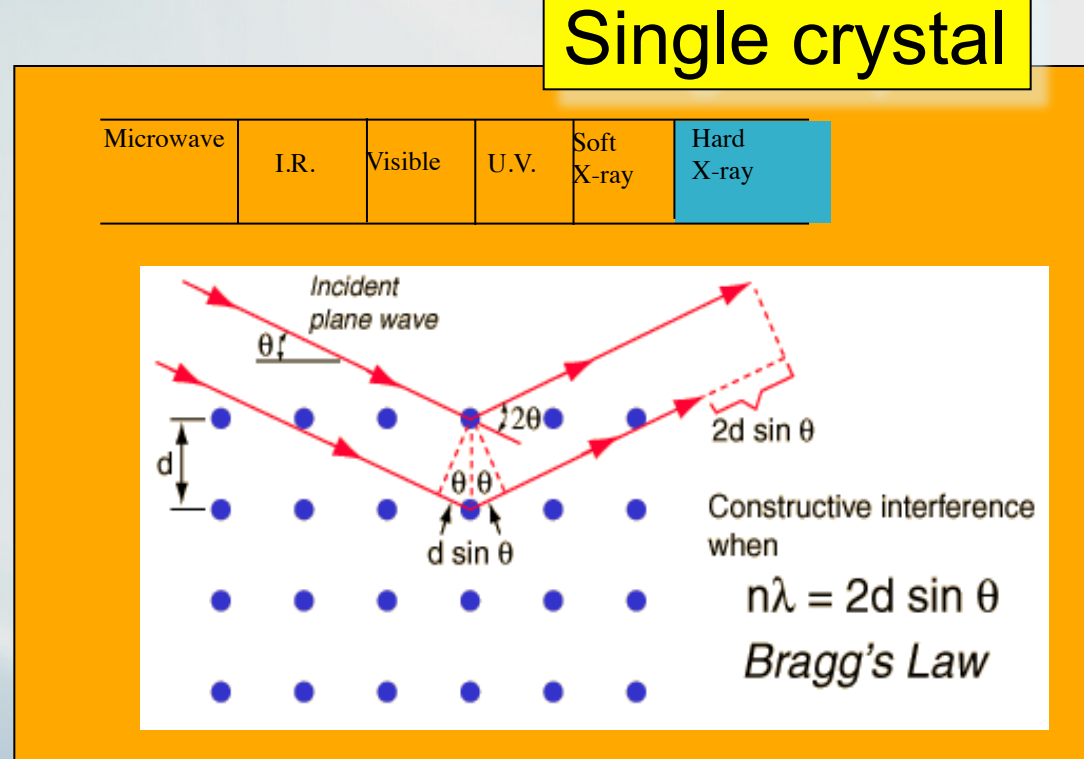
Dispersion of radiation from a bulk periodic atomic structure:
The bulk DIFFRACTION

The Bragg's law

The radiation penetrates the material and is diffused by the atoms of the structure.

The diffused waves interfere.
The interference will be constructive if the difference in optical path will be a multiple of the wavelength λ :

Single crystal





Optical component for SL: monochromators

From the Bragg's law

$$2d \sin \vartheta = n\lambda$$

therefor

$$\sin \vartheta = 1 \Rightarrow \lambda_{\max}$$

and the Bragg angle is 90°

$$\lambda_{\max} = 2d$$





Optical component for SL: monochromators

from the derivative of the Bragg's law an important property of the hard x-ray monochromators

energy resolution

$$\frac{\Delta\lambda}{\lambda} = \frac{\Delta E}{E} = \Delta\vartheta \cot g(\vartheta_B)$$

$\Delta\theta$ is the convolution of two contributes:

$\Delta\theta_{beam}$ - angular divergence of the radiation beam in the scattering plane

ω_s - the intrinsic angular bandwidth of the crystal monochromator
known as Darwin width

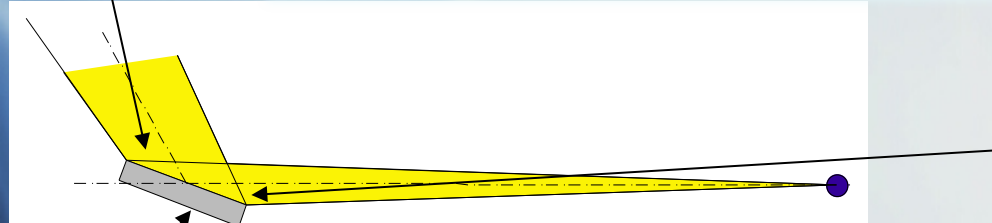


Optical component for SL: monochromators

 θ_{\min} / E_{\max}

Case with $\Delta\theta_{\text{beam}} \gg \omega_s$
white beam with divergence in the plane of scattering

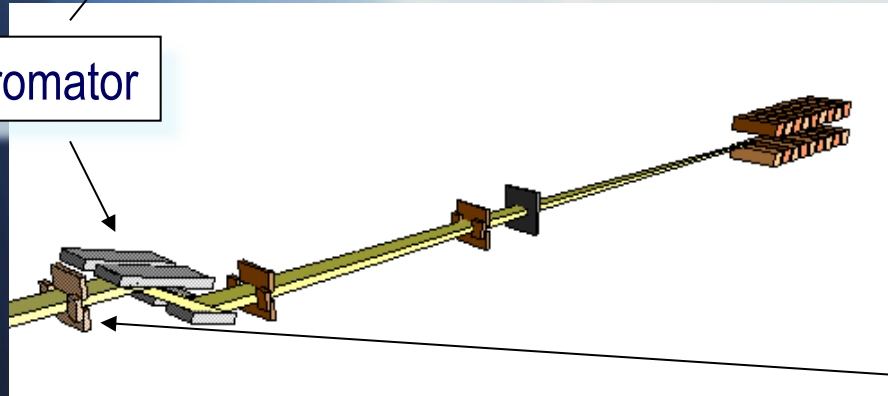
The crystal will diffract all the rays with: $\theta_{\min} \leq \theta_B \leq \theta_{\max}$



monochromator

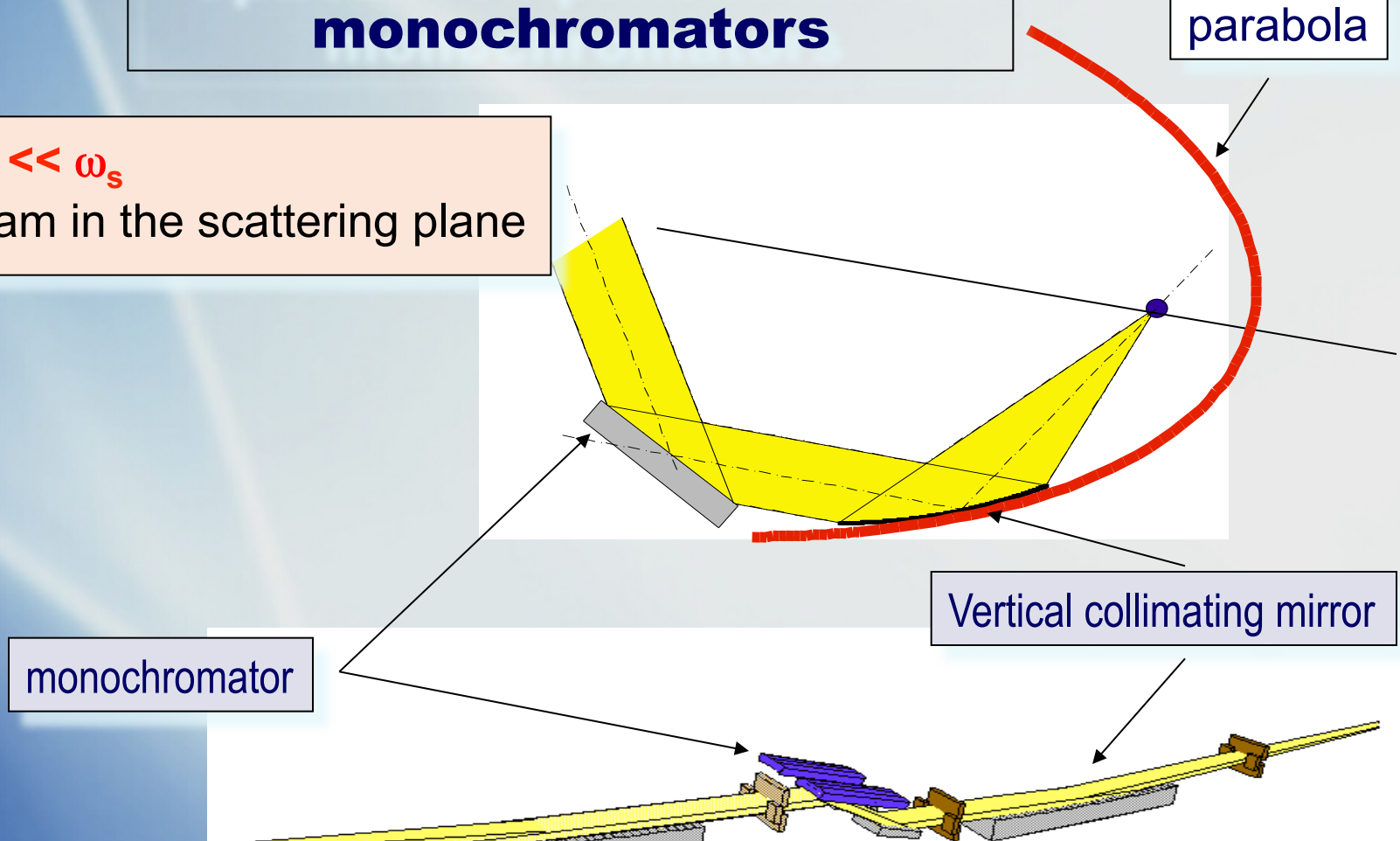
 θ_{\max} / E_{\min}

In this case the energy bandwidth is
 $\Delta E \approx \Delta\theta_{\text{beam}} \cotg(\theta_B) E$



Optical component for SL: monochromators

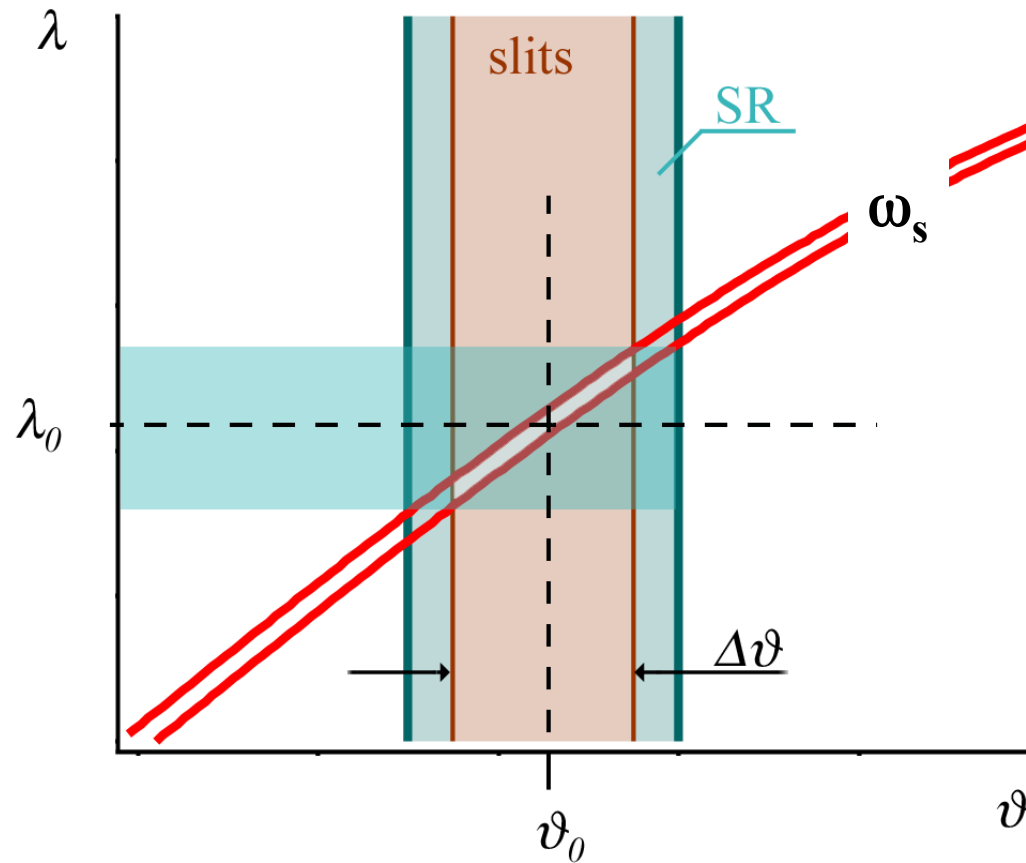
Case with $\Delta\theta_{beam} \ll \omega_s$
white parallel beam in the scattering plane



In this case the energy bandwidth will be the crystal Darwin width,
function of the Miller indexes: $\Delta E \approx \omega_s \cotg(\theta_B) E$

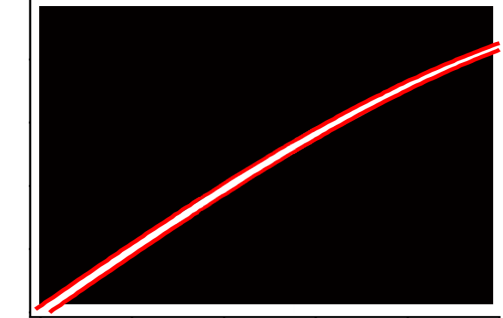
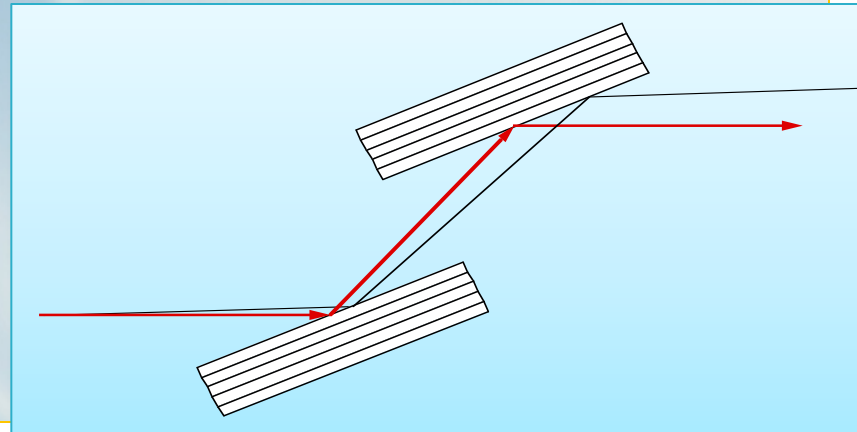
Optical component for SL: monochromators

Dumond's diagram

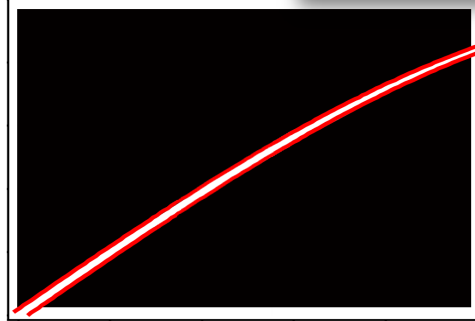


Optical component for SL: Hard x-rays monochromators

Second crystal in ***non dispersive*** configuration to achieve a fixed exit beam



Dumond diagram of the second crystal

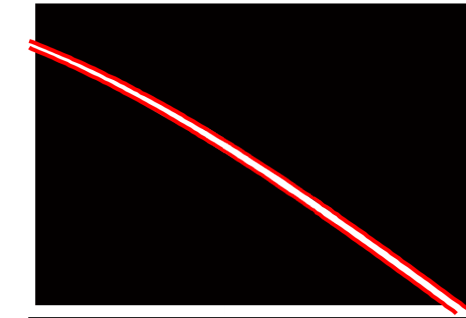
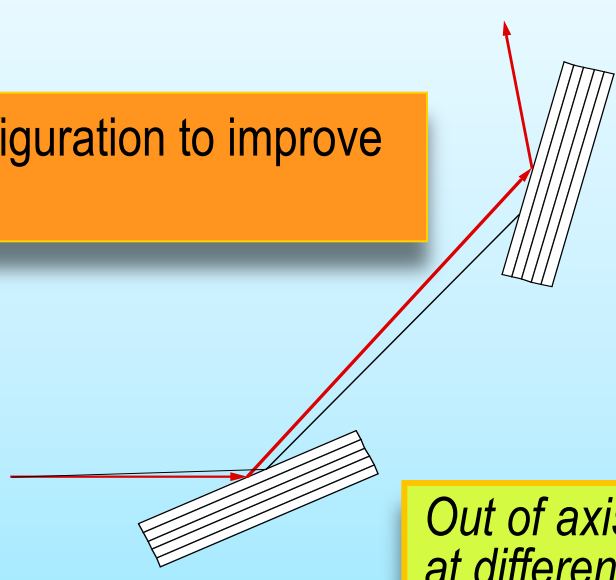


Dumond diagram of the first crystal

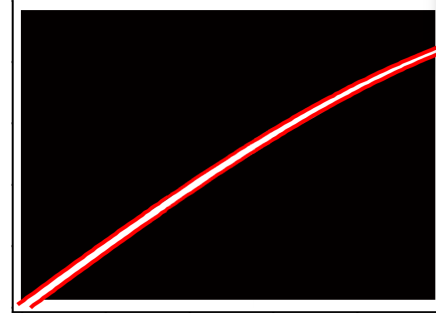
All rays accepted by the first crystal are accepted also at the second one

Optical component for SL: Hard x-rays monochromators

Second crystal in **dispersive** configuration to improve energy resolution

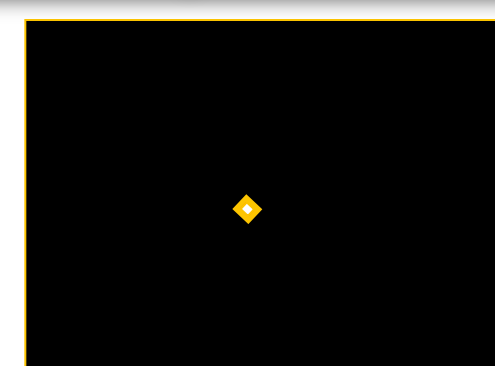


Dumond diagram of the second crystal



Dumond diagram of the first crystal

Out of axis rays on the first crystal are incident at different angles on the second one.



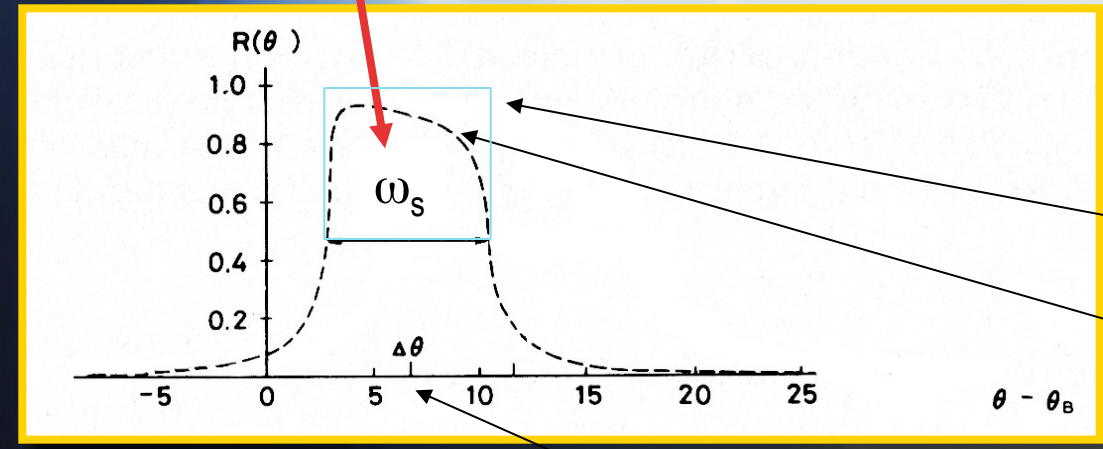
Dumond diagram of both crystals

INTENSITY OF THE REFLECTION

- reflectivity or peak reflectivity
- integral reflecting power

The Darwin curve

$$\omega_s = \frac{2}{\sin 2\theta_B} \frac{r_e \lambda_1^2}{\pi V} C |F_{hr}| e^{-M(n)}$$



n	order of the reflection
λ_1	wavelength of the fundamental
$e^{-M(n)}$	temperature factor
V	volume of the unit cell
θ_B	Bragg angle
R_e	radius of the electron e^2/mc^2
F_{hr}	real part of the structure factor related to the diffracted direction $h(h,k,l)$

predicted by the dynamical theory

absorption effects

angular shift due to the refractive effect



the **b** parameter
defined as :

$$b = \frac{\sin(\alpha - \vartheta_B)}{\sin(\alpha + \vartheta_B)}$$

a is the angle between the Bragg plane and the crystal surface

T. Matsushita and H. Hashizume *X-Ray Monochromators*
Handbook on Synchrotron Radiation, Vol. 1

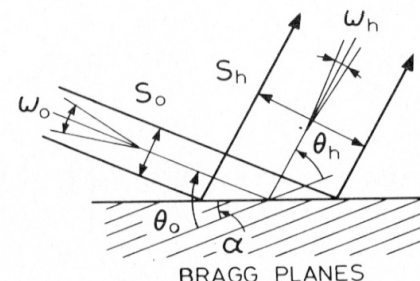


Fig. 3. Geometry of X-ray reflection by a perfect single crystal. θ_0 : incidence angle; θ_h : reflection angle. For a non-zero asymmetry angle α ($0 < |\alpha| < \theta_B$), the angular width ω_0 for acceptance is not equal to the angular width ω_h for emergence. The figure is drawn for $b < 1.0$, where $\omega_0 > \omega_s > \omega_h$. Note also the change of beam cross sections, S_0 and S_h .

$$\omega_0 = \frac{\omega}{\sqrt{b}}$$

the angular acceptance as
function of the intrinsic width
and the **b** parameter:



T. Matsushita and H. Hashizume **X-Ray Monochromators**
Handbook on Synchrotron Radiation, Vol. I

Bragg reflection width in case of asymmetric cut crystal is defined by:

$$\omega_h = b\omega_o$$

the angular acceptance as function of the Bragg reflection width

also for the beams sections

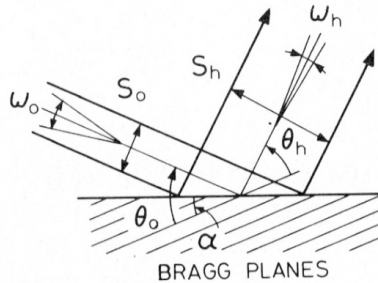


Fig. 3. Geometry of X-ray reflection by a perfect single crystal. θ_0 : incidence angle; θ_h : reflection angle. For a non-zero asymmetry angle α ($0 < |\alpha| < \theta_B$), the angular width ω_0 for acceptance is not equal to the angular width ω_h for emergence. The figure is drawn for $b < 1.0$, where $\omega_0 > \omega_s > \omega_h$. Note also the change of beam cross sections, S_0 and S_h .

$$\omega_h = \omega_s \sqrt{b}$$

$$S_h = \frac{S_o}{b}$$

combining the two formulas we have the well known Liouville's theorem

$$\omega_h S_h = \omega_o S_o$$



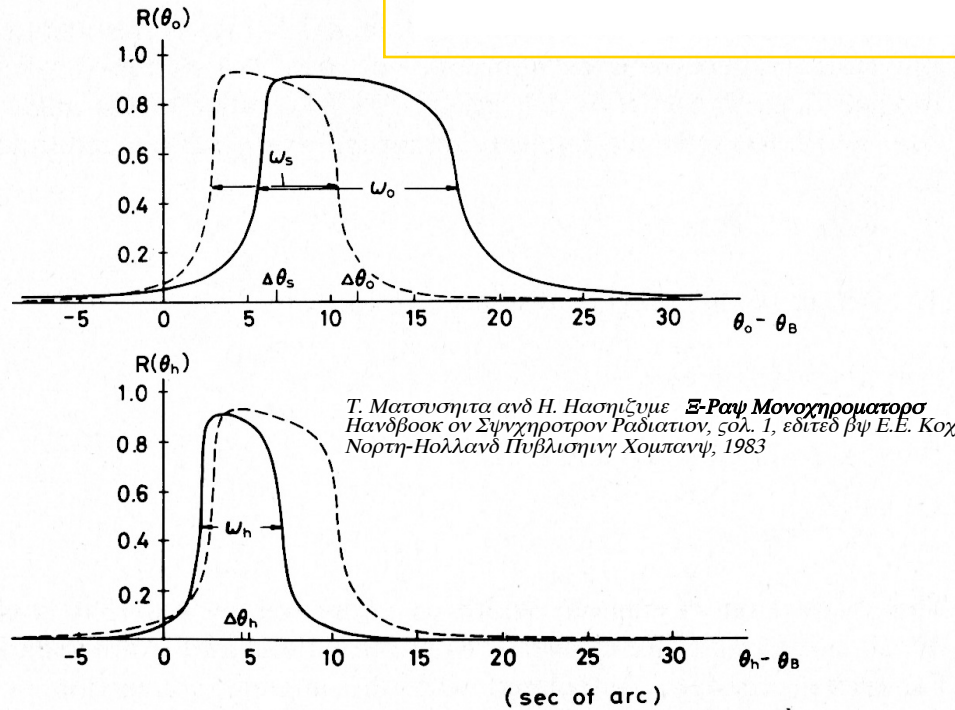
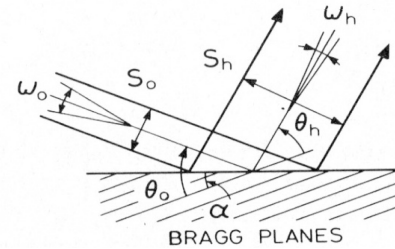


Fig. 4. Perfect-crystal reflection curves for the (111) reflection of silicon at 1.6 \AA . $R(\theta_0)$ shows the reflectivity for the ideal plane wave as a function of the incidence angle θ_0 , while $R(\theta_h)$ represents the intensity reflected at a reflection angle θ_h for a plane wave incident at θ_0 , θ_0 and θ_h being related by $(\theta_h - \theta_B) = b(\theta_0 - \theta_B)$. The solid curves are calculated for an asymmetric case of $b = 0.4$, while the broken curves for the symmetric case ($b = 1.0$) where $R(\theta_0) \equiv R(\theta_h)$.



T. Matsushita and H. Hashizume X-Ray Monochromators
Handbook on Synchrotron Radiation, Vol. 1

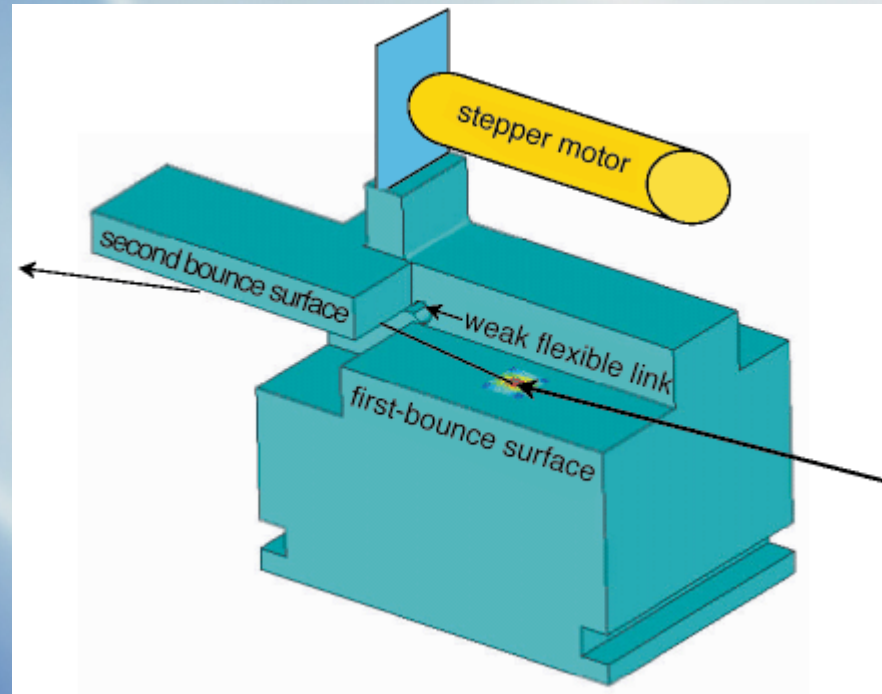
Table 2
Intrinsic Bragg reflection widths ω_s , energy resolutions $\Delta E/E$ and integral reflecting powers I of perfect crystals of silicon, germanium and α -quartz at 1.54 Å.

Crystal	hkl	ω_s (second or arc)	$\Delta E/E$ ($\times 10^5$)	I ($\times 10^6$)
Silicon	111	7.395	14.1	39.9
	220	5.459	6.04	29.7
	311	3.192	2.90	16.5
	400	3.603	2.53	19.3
	331	2.336	1.44	11.8
	422	2.925	1.47	15.5
	333			
	(511)	1.989	0.88	9.9
	440	2.675	0.96	14.0
	531	1.907	0.60	9.3
Germanium	111	16.338	32.64	85.9
	220	12.449	14.46	67.4
	311	7.230	6.92	37.1
	400	7.951	5.94	42.3
	331	5.076	3.34	25.4
	422	6.178	3.34	32.4
	333			
	(511)	4.127	2.00	20.2
	440	5.339	2.14	27.5
	531	3.719	1.33	17.7
α -quartz	100	3.798	10.00	18.8
	101	7.453	15.26	40.9
	110	2.512	3.69	12.2
	102	2.488	3.36	12.9
	200	2.252	2.81	11.5
	112	2.927	3.03	15.5
	202	2.072	1.93	10.6
	212	2.042	1.47	10.7
	203	2.430	1.74	12.9
	301	2.368	1.69	12.6





The simplest DCM, the **channel-cut**



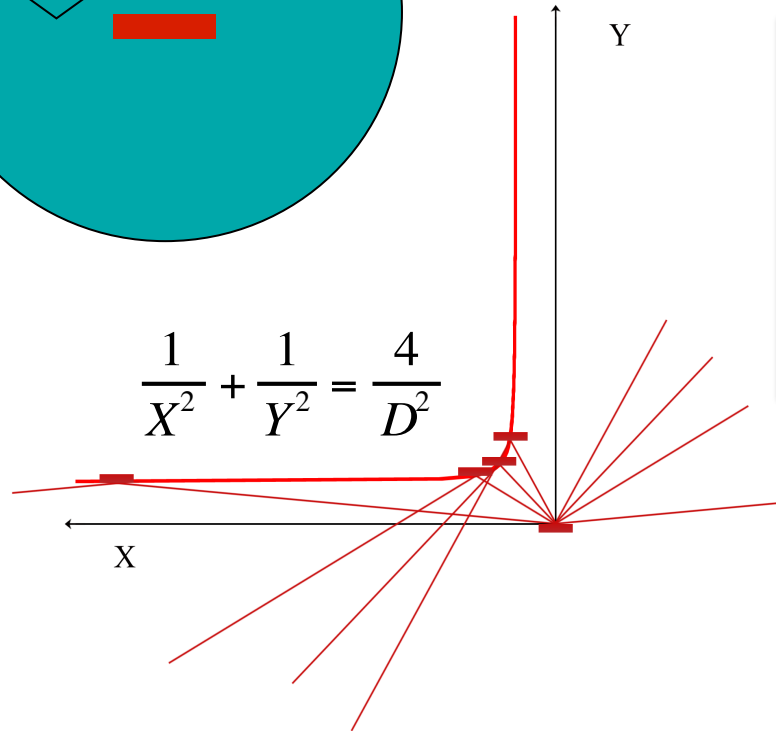
The channel-cut DCM is made from a single crystal monolith.
Advantages: simple, intrinsically aligned
Disadvantages: not fixed height beam output changing the energy





Pseudo channel-cut Double Crystal Monochromator

$$\frac{1}{X^2} + \frac{1}{Y^2} = \frac{4}{D^2}$$



The pseudo channel-cut DCM is made from two single crystals mounted on to a common rotating table.

Advantages:

fixed height beam output changing the energy

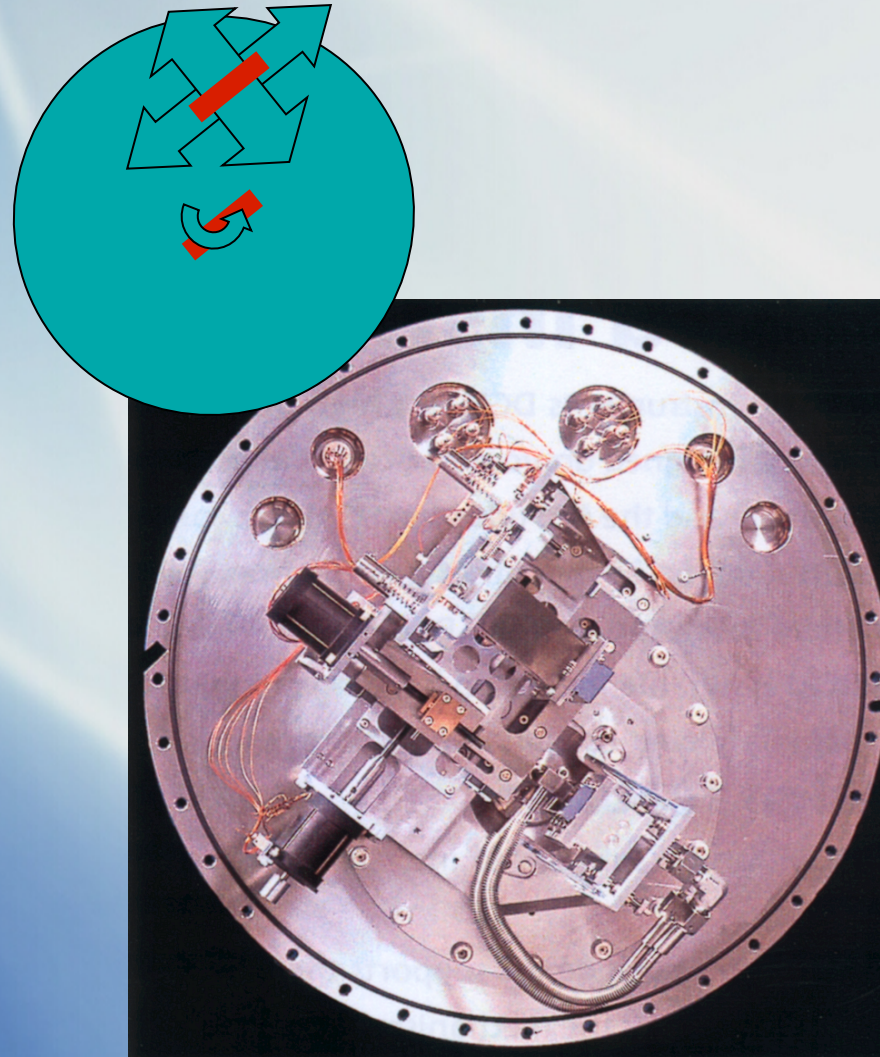
Disadvantages:

it needs coarse and fine regulations for the second crystal



Elettra
Sincrotrone
Trieste

Pseudo channel-cut Double Crystal Monochromator



Edoardo Busetto & Luca Rebuffi - MVO Group
Elettra - Sincrotrone Trieste S.C.p.A.

ICTP, Grignano (TS), 07/05/2018





Independent Double Crystal Monochromator

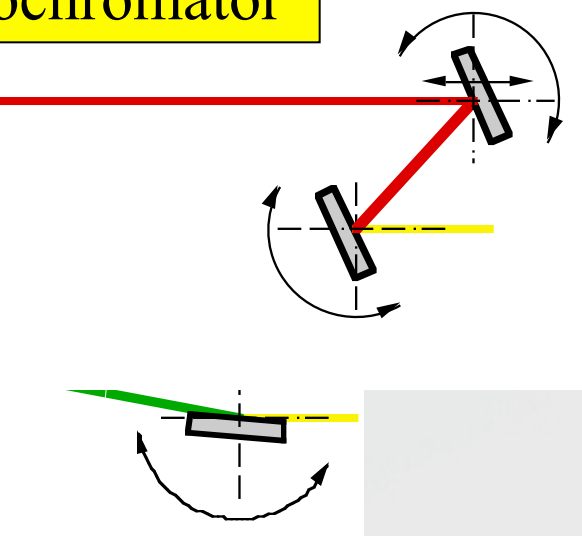


Si(111)
crystal positions:

- 2100 eV $\theta = 70.3^\circ$
- 2300 eV $\theta = 59.3^\circ$
- 25000 eV $\theta = 4.5^\circ$

II crystal movements:

- II crystal translation
- II crystal rotation
- linear slide



The first crystal can rotate. The second crystal can rotate and translate.

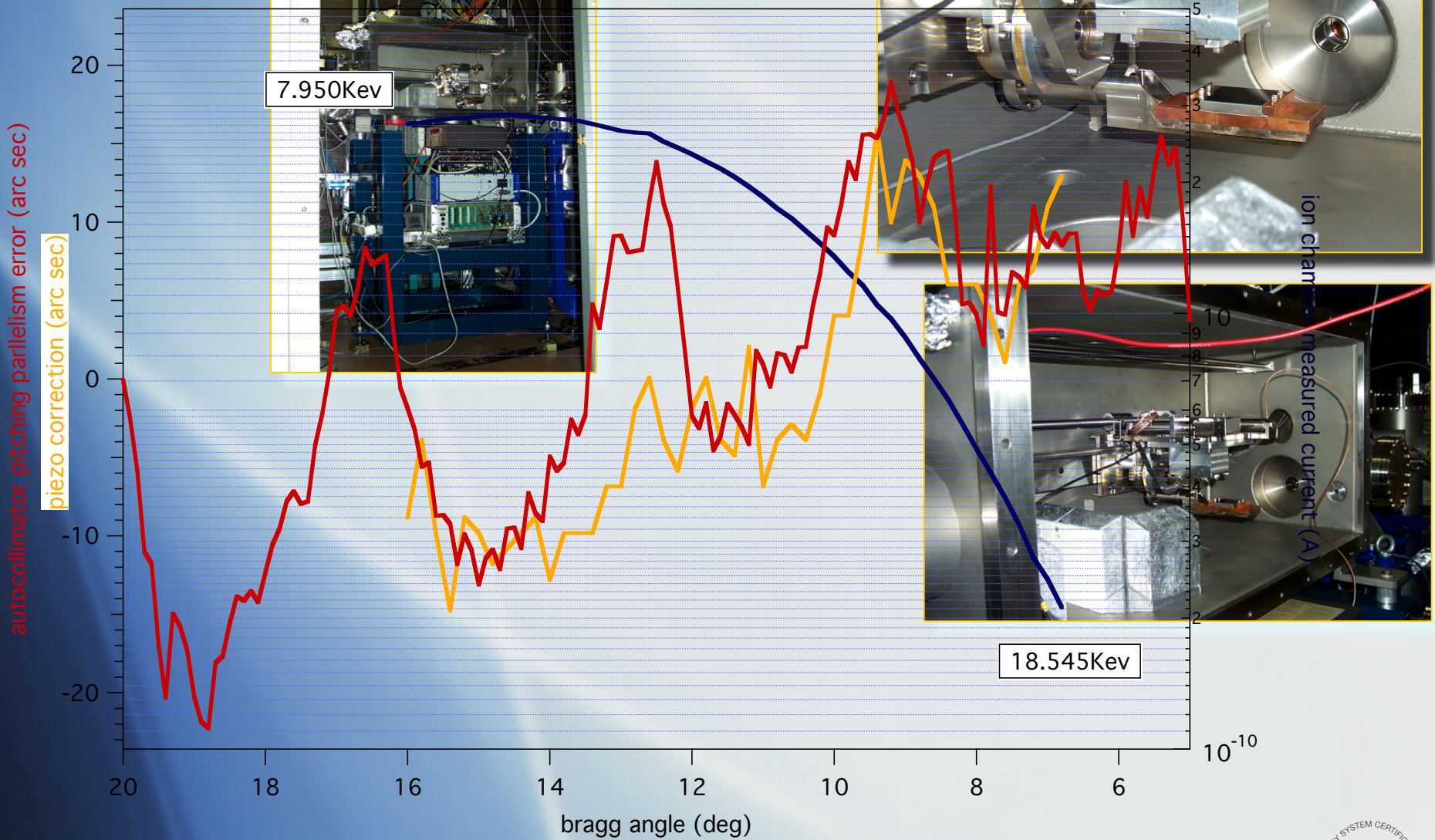
Advantages:

fixed height beam output due to the mechanical construction along a wide energy range
it needs coarse and fine regulations for the second crystal

Disadvantages:



Elettra
Sincrotrone
Trieste



Edoardo Busetto & Luca Rebuffi - MVO Group
Elettra - Sincrotrone Trieste S.C.p.A.

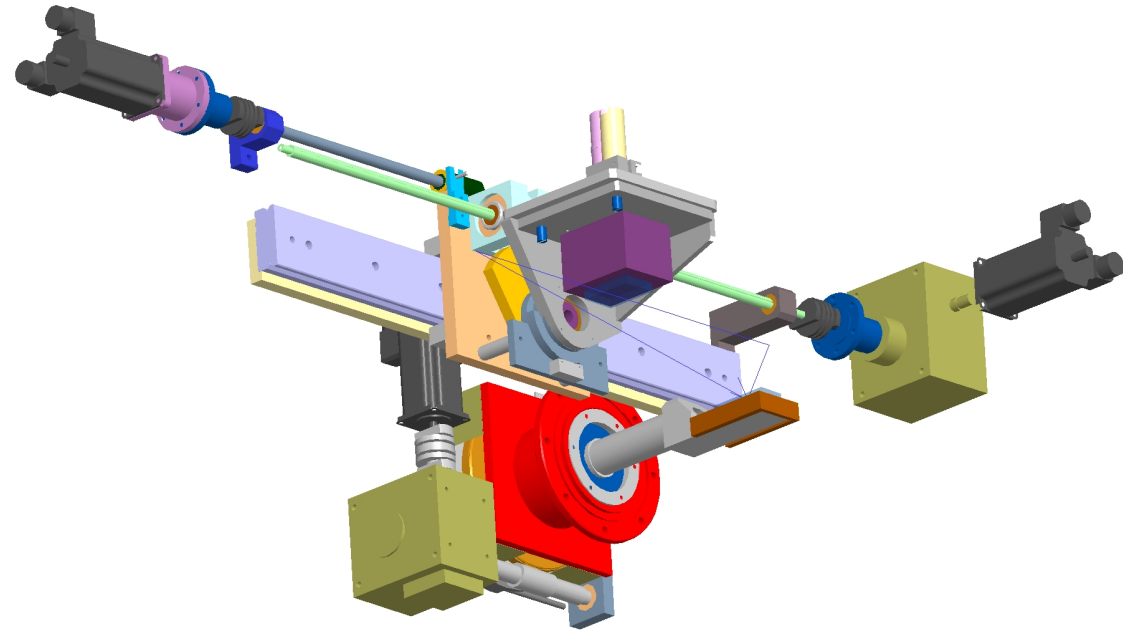
ICTP, Grignano (TS), 07/05/2018





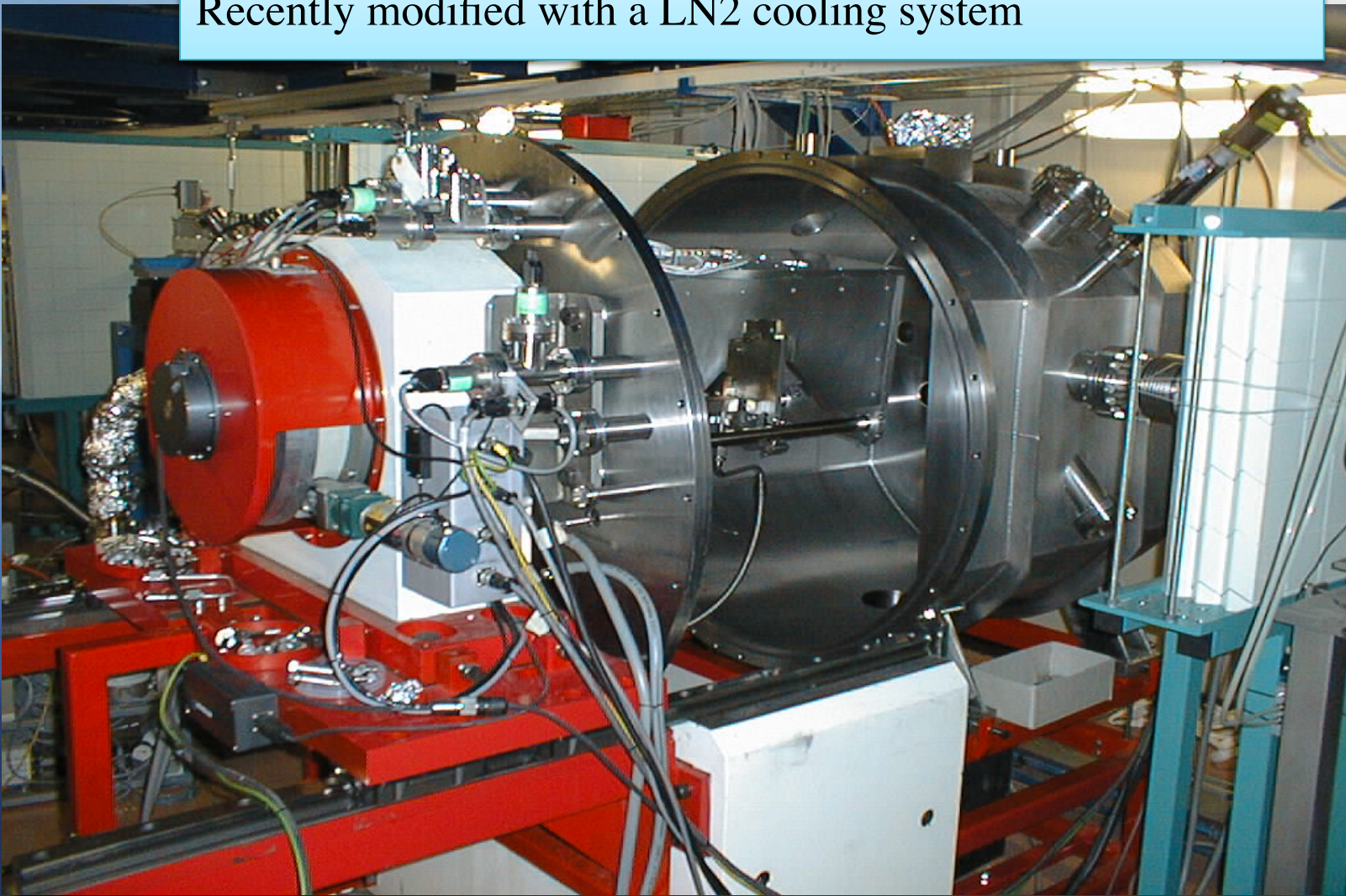
Final design 3D view

The monochromar equipped with a sagittal bender
is operating at the powder diffraction beamline @ Elettra





The XRD1 Double Crystal monochromator @ Elettra
it has been designed in Elettra in 1991. It operates since 1994.
Recently modified with a LN2 cooling system



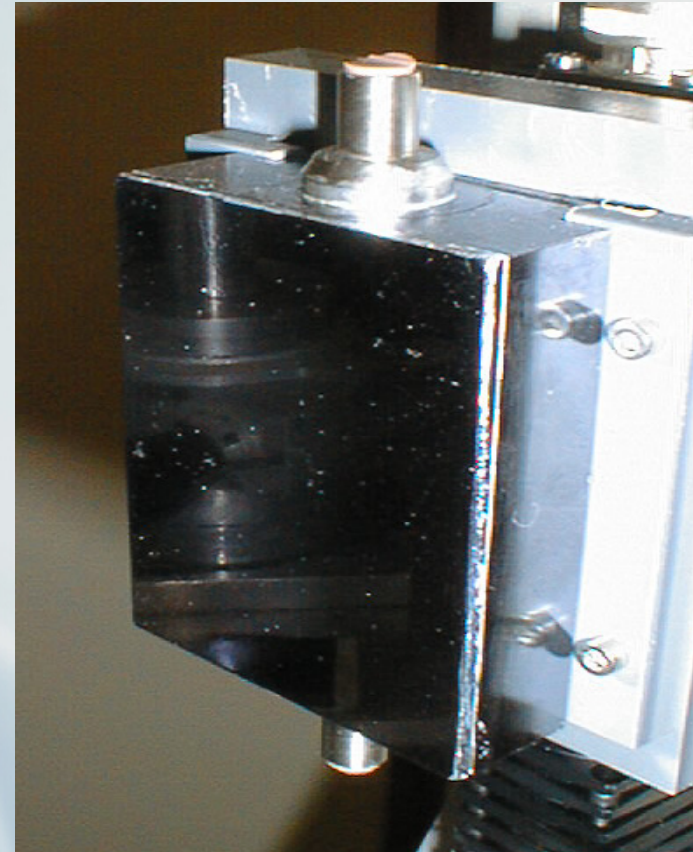


Elettra
Sincrotrone
Trieste

Monochromator optics and thermal load XRD1

Absorbrd power 0.4 kW*

* $1.5 \times 0.28 \text{ mrad}^2$



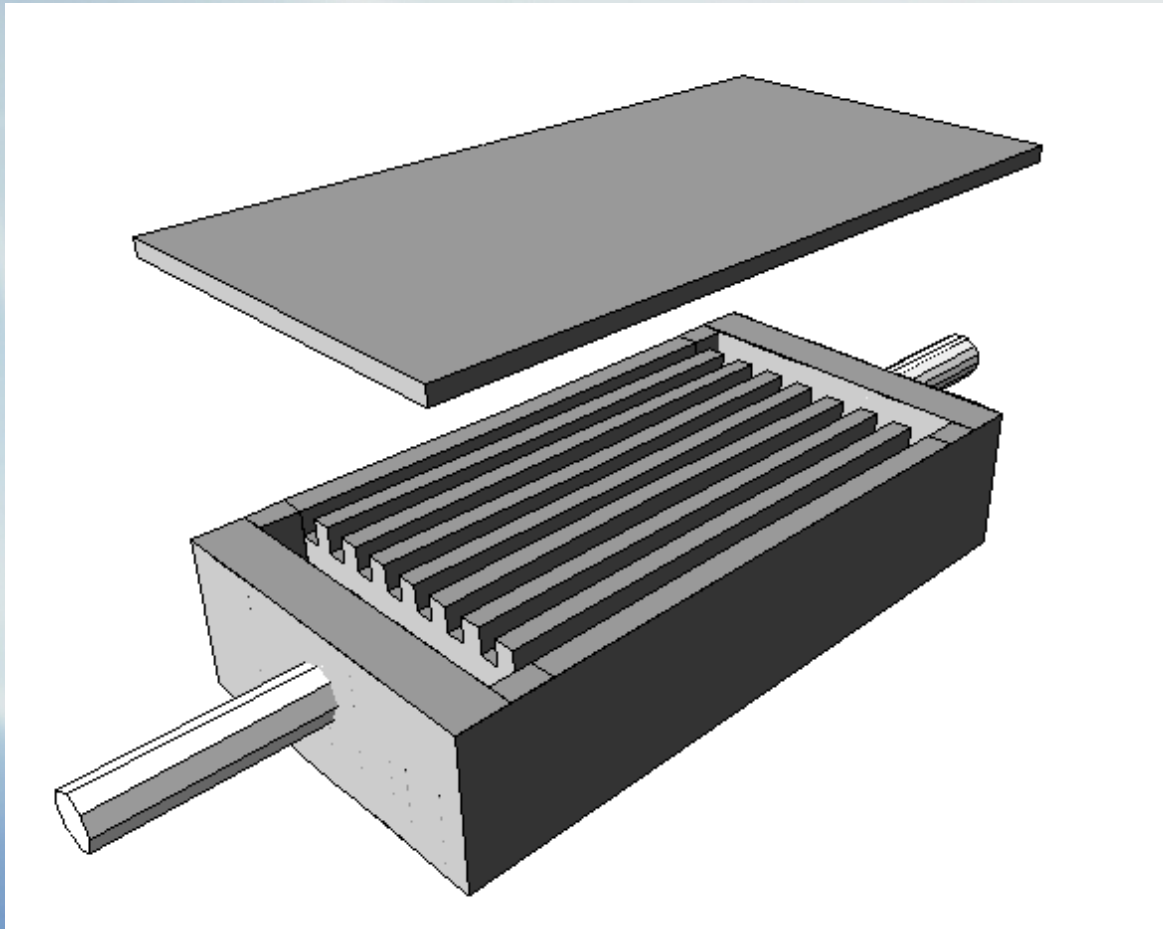
Edoardo Busetto & Luca Rebuffi - MVO Group
Elettra - Sincrotrone Trieste S.C.p.A.

ICTP, Grignano (TS), 07/05/2018





Elettra
Sincrotrone
Trieste



Edoardo Busetto & Luca Rebuffi - MVO Group
Elettra - Sincrotrone Trieste S.C.p.A.

ICTP, Grignano (TS), 07/05/2018





The two crystal elements before brazing in vacuum oven (first prototype)

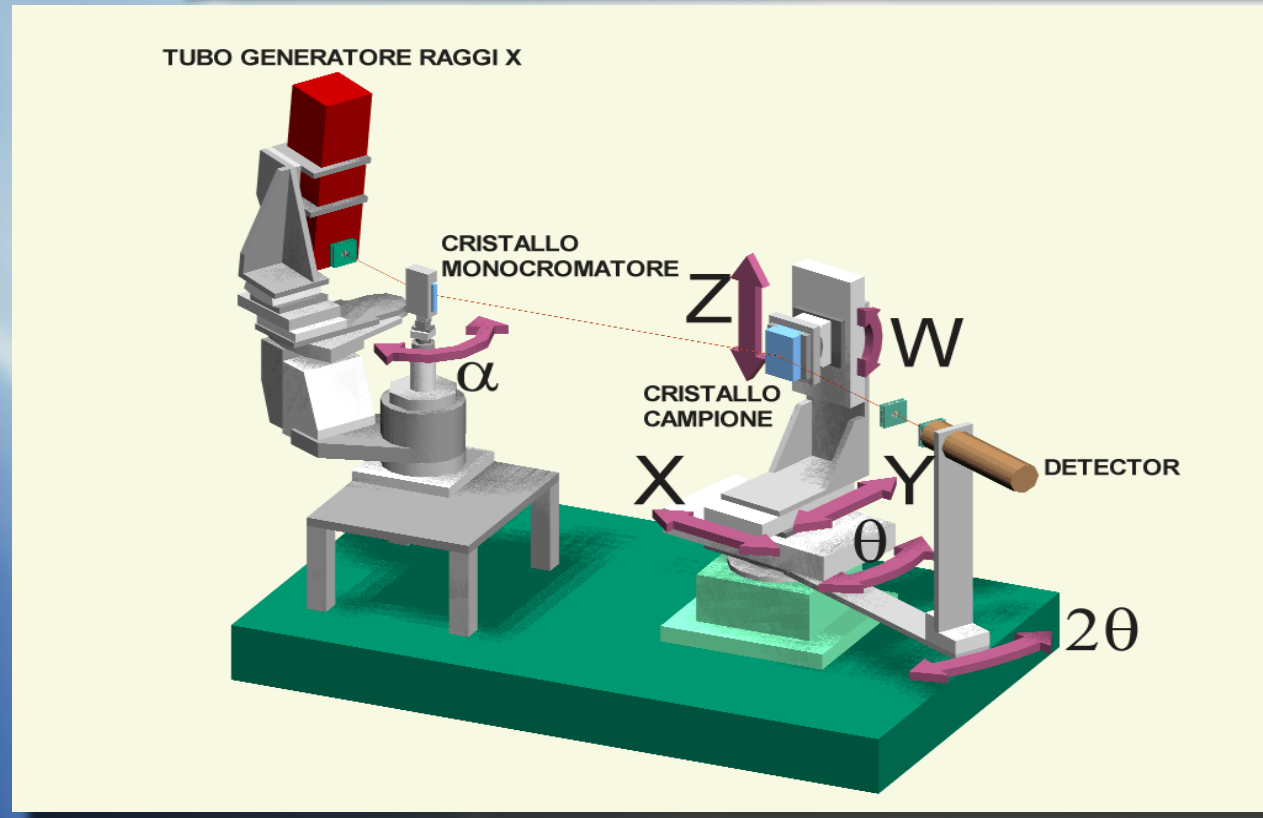


Channels

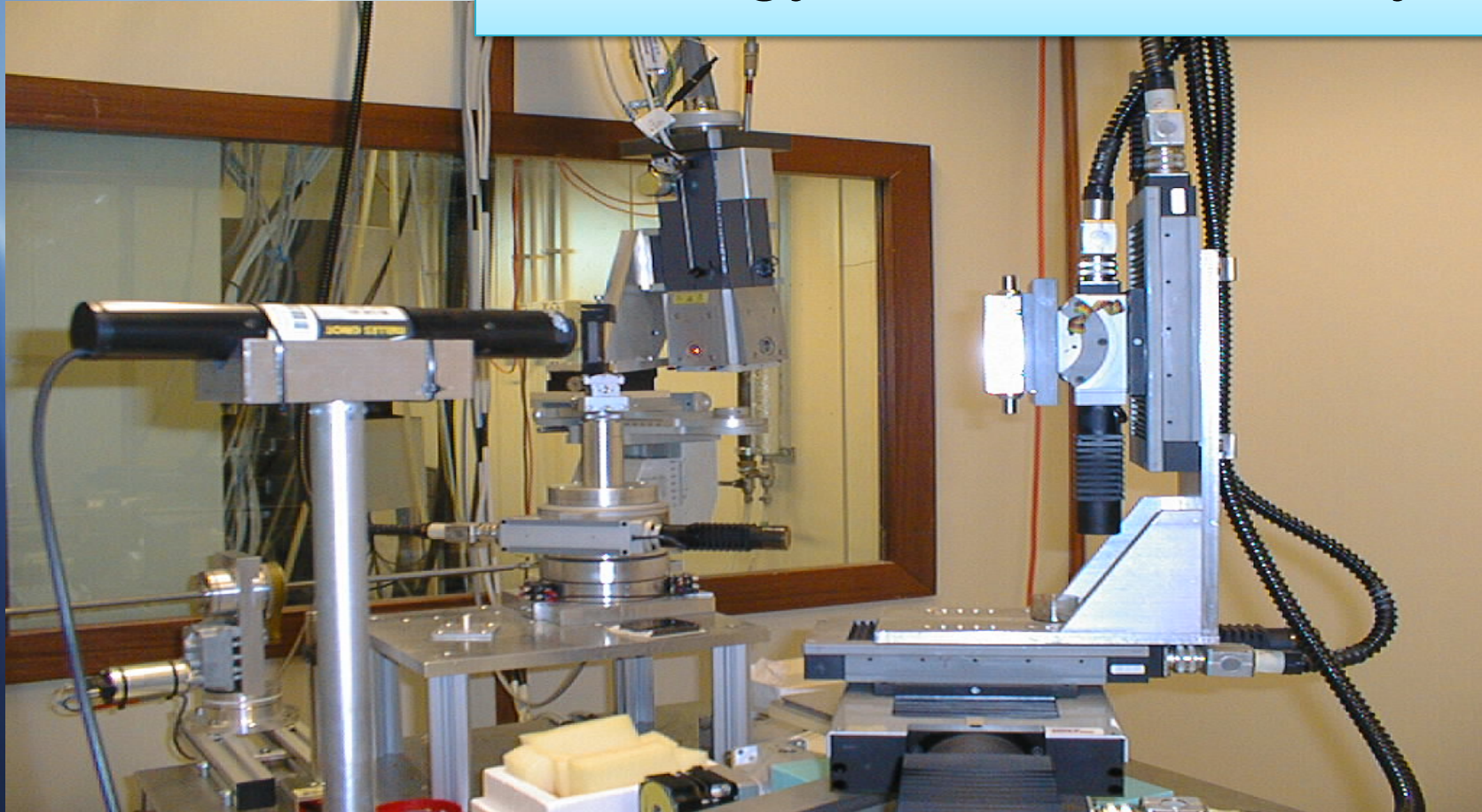
thickness:
depth:

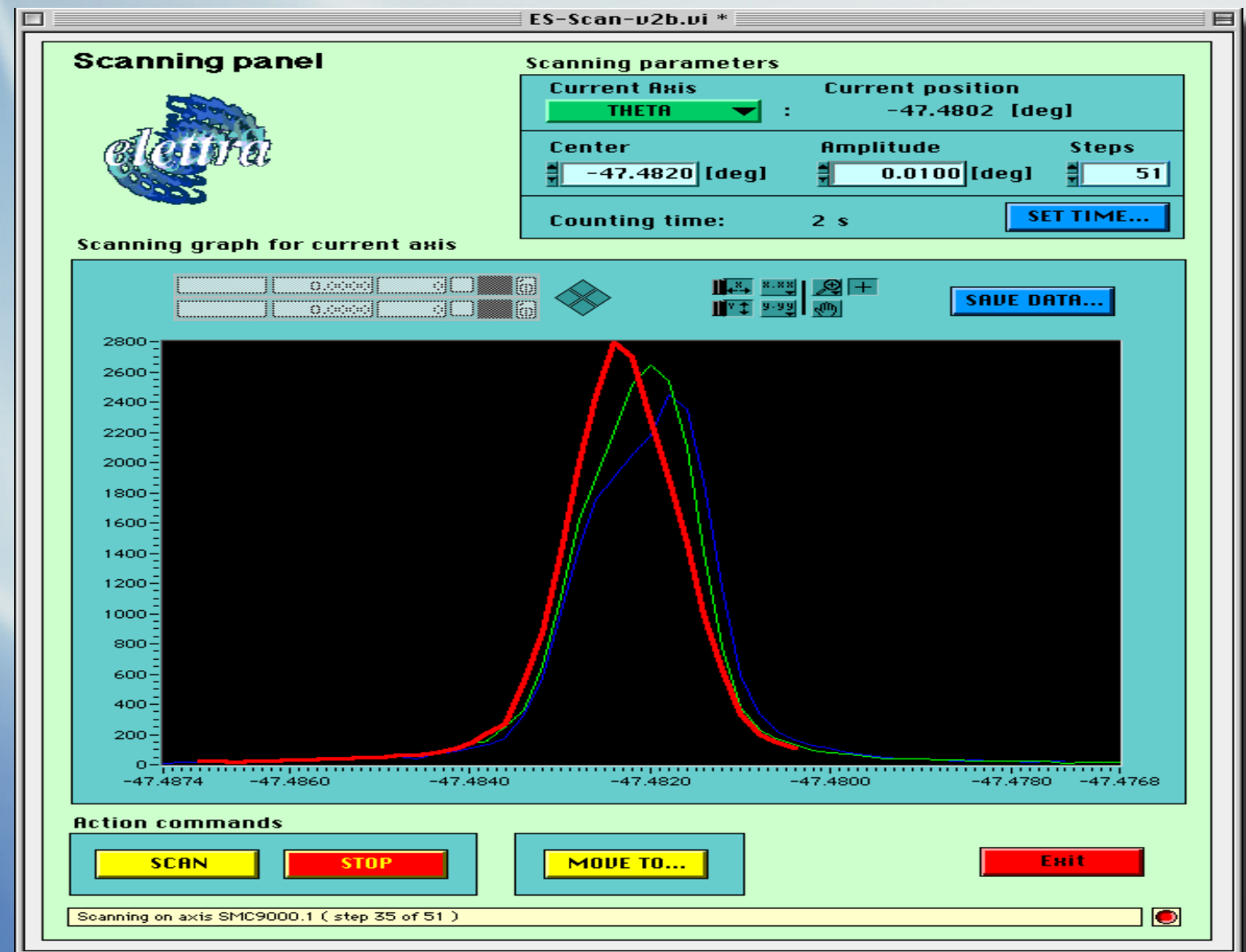
$300 \mu\text{m}$
2 mm

Metrology station with X-rays



Metrology station with X-rays

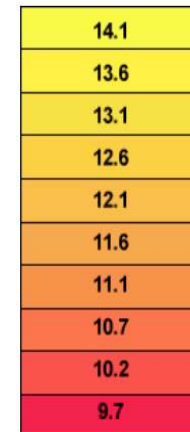
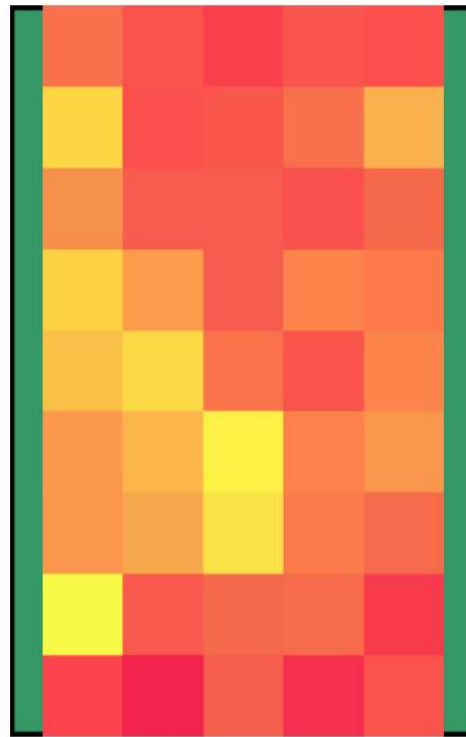






Rasterized crystal point rocking curve @ 1.54 Å Si111 FWHM 10.3 arcsec.

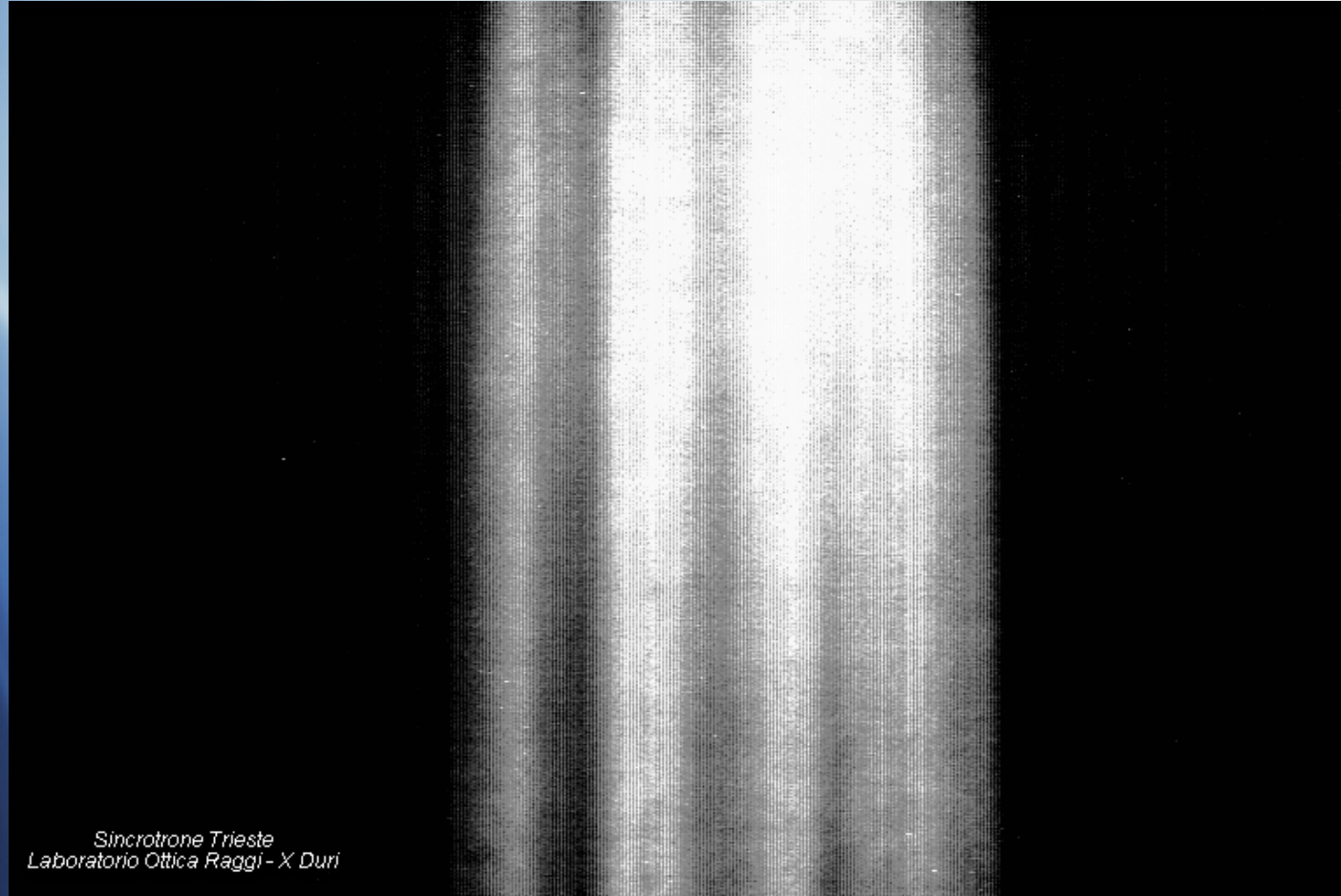
DISTRIBUZIONE DELL'AMPIEZZA DELLE ROCKING-CURVE
VALUTATE MEDIANTE DIFFRAZIONE SUI PIANI Si-111



Valori espressi in
secondi di grado



Topography of the internal cooled Si-crystal with channels perpendicular to the scattering plane



Sincrotrone Trieste
Laboratorio Ottica Raggi-X Duri



Edoardo Busetto & Luca Rebuffi - MVO Group
Elettra - Sincrotrone Trieste S.C.p.A.

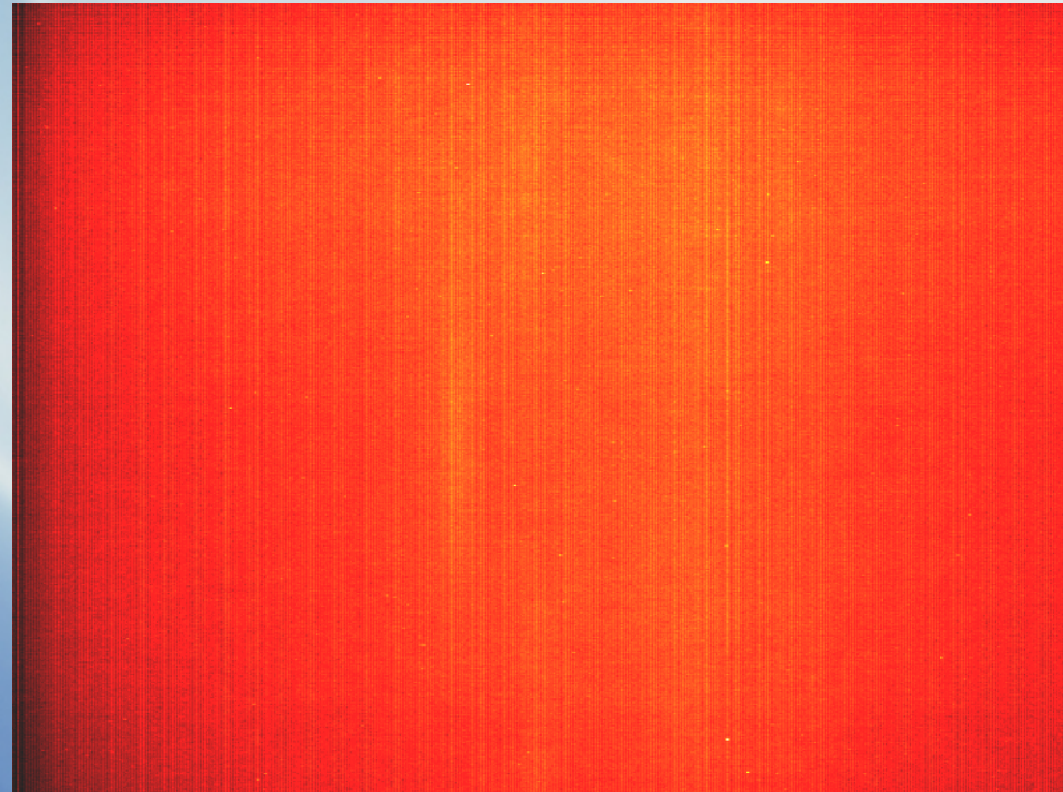
ICTP, Grignano (TS), 07/05/2018





Elettra
Sincrotrone
Trieste

Topography live



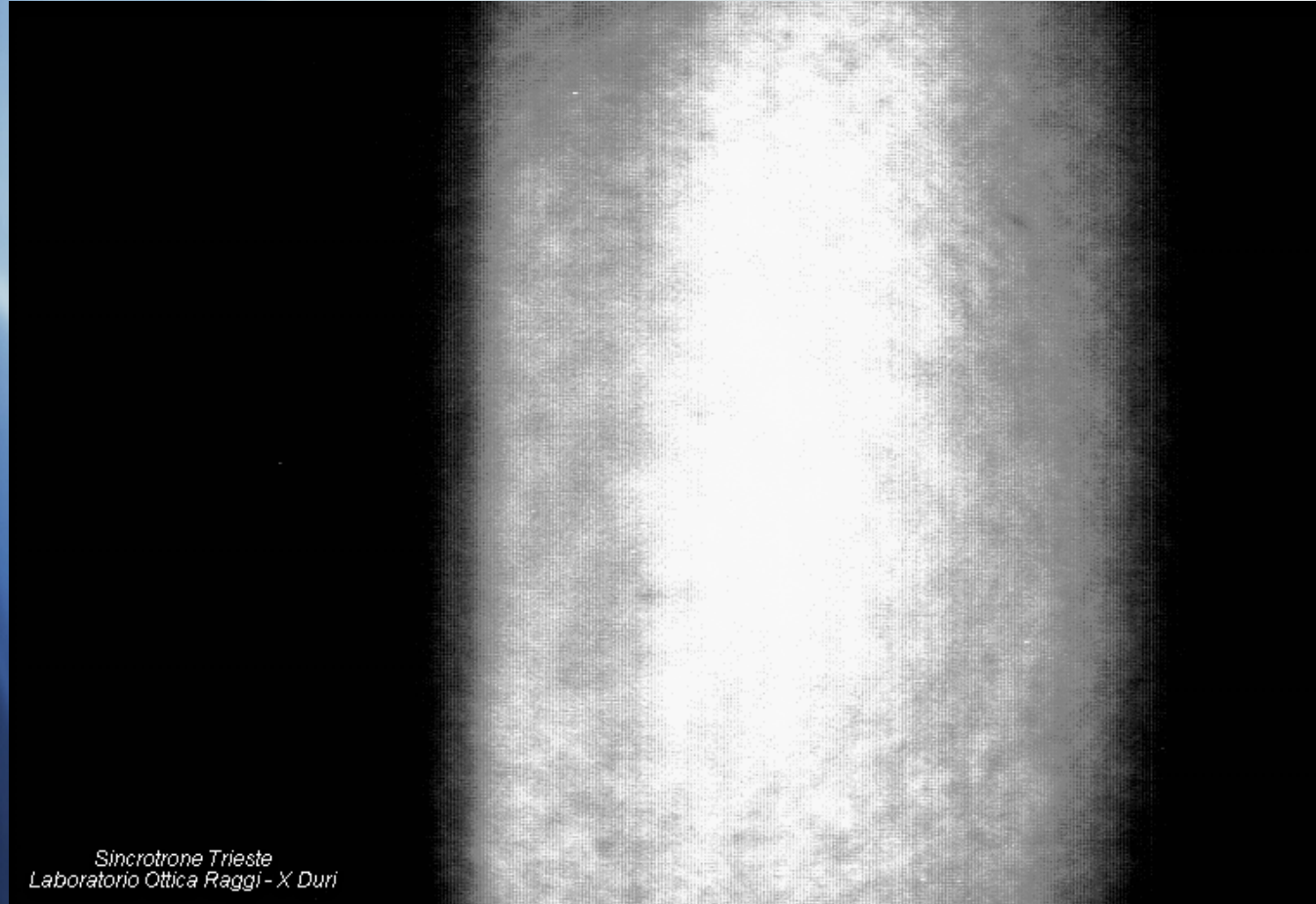
Edoardo Busetto & Luca Rebuffi - MVO Group
Elettra - Sincrotrone Trieste S.C.p.A.

ICTP, Grignano (TS), 07/05/2018





Same topography but with channels in the same direction of the scattering plane



Sincrotrone Trieste
Laboratorio Ottica Raggi - X Duri





- Detector for Hard X-rays

- Two large families:

single counters
integrators





■ Single counters :

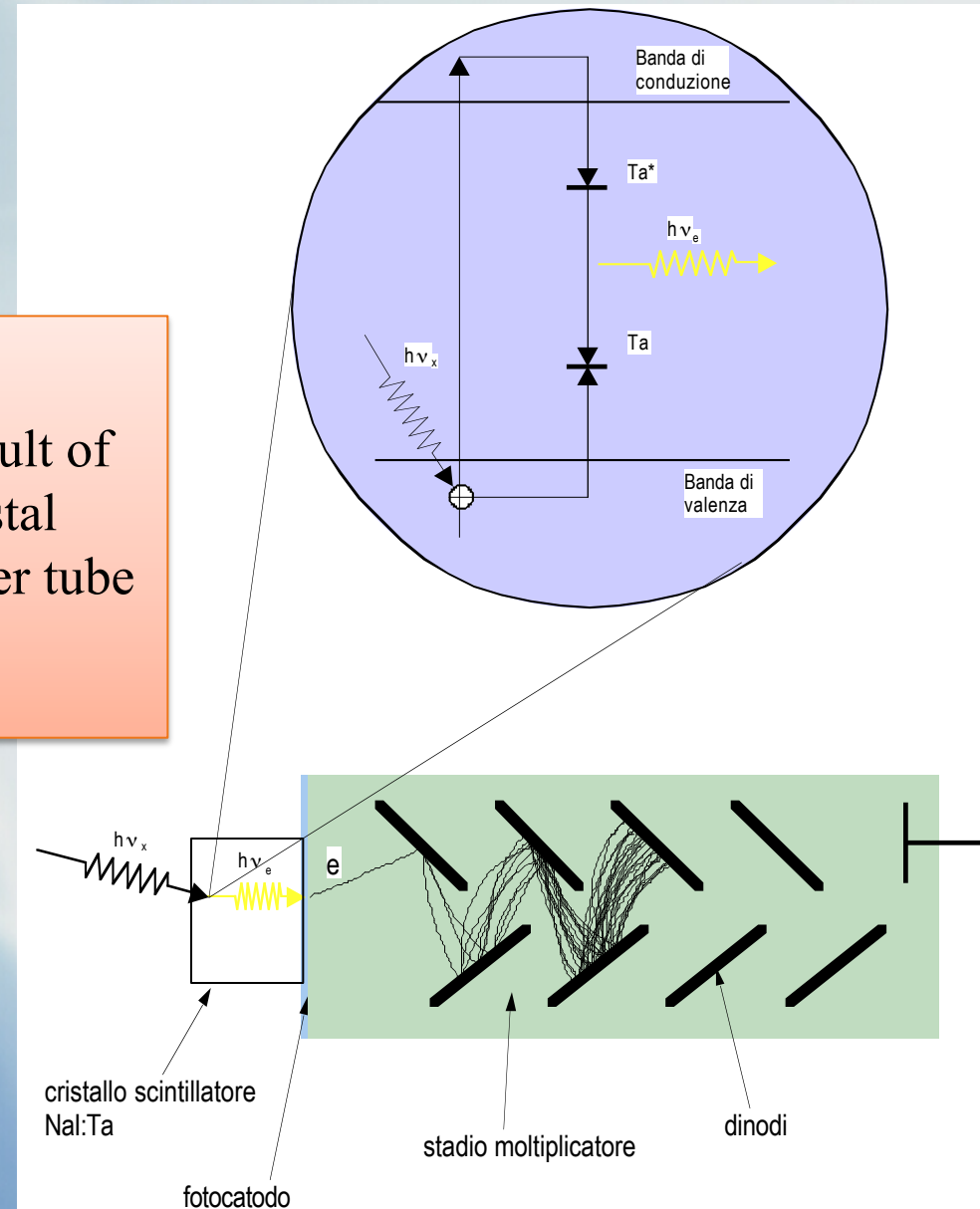
- These systems allow to collect all the electrons produced by the absorption of an x-ray.
- The mean number of electrons produced during the absorption process is proportional to energy of the single x-ray.
- Used in spectroscopy



Scintillators

These kind of detectors are the result of the coupling between a doped crystal (i.e. NaI:Ta) and a photo-multiplier tube

https://en.wikipedia.org/wiki/Scintillation_counter





2D Integrators detectors

- They integrates the charge. Generally losing the direct correlation between electrons produced and energy of the absorbed photon.
- The signal local intensity has to be proportional to the dose absorbed in the same region.
- Correlation is possible in case of monochromatic beam





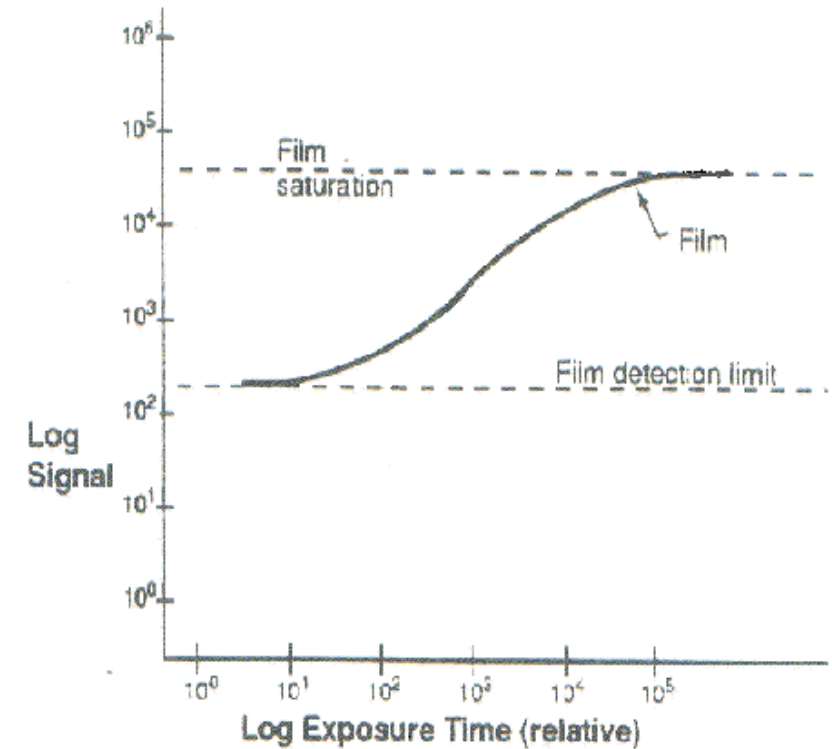
Radiographic film (totally analogic)

It is still one of the most used detector.
Due to the photocemical reaction $\text{AgBr} \rightarrow \text{Ag}^+$ with a density of Ag^+ that is proportional to the absorbed radiation. The developer bath reduces $\text{Ag}^+ \rightarrow \text{Ag}$ with the tipical gray scale we are used to see .

Characteristic curve of the film density versus the time exposure (log/log)

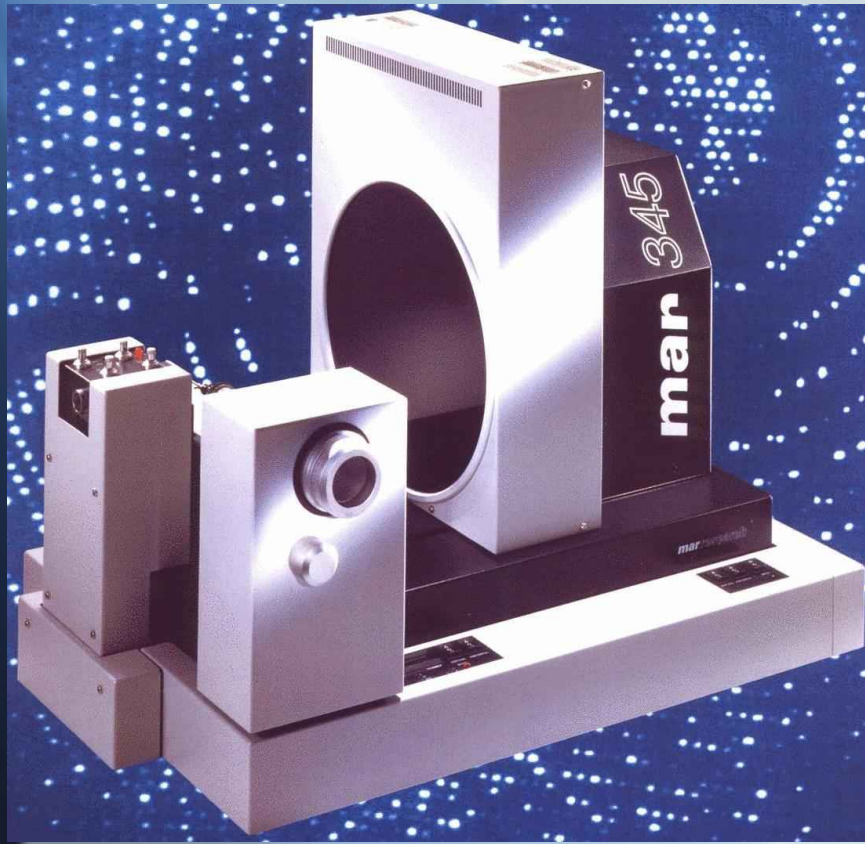
Dynamic range
Linearity

Linearità e range dinamico delle emulsioni fotografiche

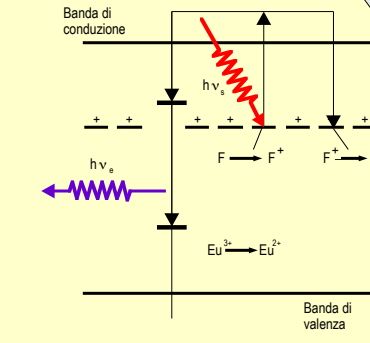
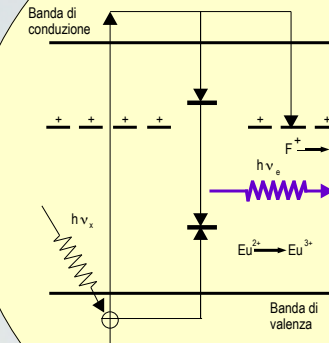
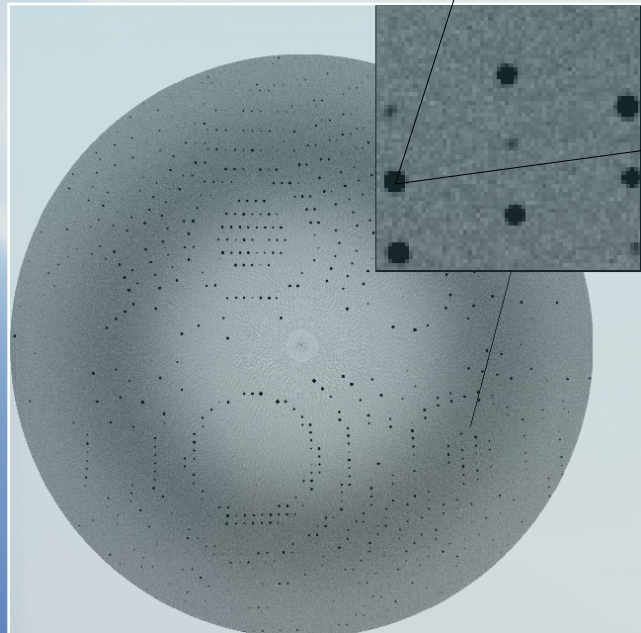




2D integrator detectors (analog/digital)



Imaging Plate... analogical detector with digital readout





Elettra
Sincrotrone
Trieste

2D integrator detectors (totally digital)



Edoardo Busetto & Luca Rebuffi - MVO Group
Elettra - Sincrotrone Trieste S.C.p.A.

ICTP, Grignano (TS), 07/05/2018





PILATUS 6M: Specifications

No of Modules: 60

Module arrangement: 5 x 12

Detector Size: 431 x 448 mm²

Format: 2527 x 2463 pixels

Spatial resolution: 0.172 x 0.172 mm²

Dynamic range/pixel: 20bits

Count rate/pixel: <8 Mcps/pixel

Readout time: 3.5 ms

Frame rate: 12.5 Hz

Compressed dimension: ≈ 6M/frame

Mechanical positioning: Flat geometry

Intermodule gap x: 7 pixels, y: 17 pixels, 8.4% of total area



Data storage?..... Hops! we have a problem!





Elettra
Sincrotrone
Trieste

THANK YOU!



Edoardo Busetto & Luca Rebuffi - MVO Group
Elettra - Sincrotrone Trieste S.C.p.A.

ICTP, Grignano (TS), 07/05/2018

